(2)

MEMORANDUM REPORT BRL-MR-3888

BRL

IN-FLIGHT PRESSURE MEASUREMENTS ON SEVERAL 155MM, M864 BASE BURN PROJECTILES

LYLE D. KAYSER
JOHN D. KUZAN
DAVID N. VAZQUEZ

JANUARY 1991

U.S. ARMY LABORATORY COMMAND

BALLISTIC RESEARCH LABORATORY
ABERDEEN PROVING GROUND, MARYLAND

NOTICES

Destroy this report when it is no longer needed. DO NOT return it to the originator.

Additional copies of this report may be obtained from the National Technical Information Service, U.S. Department of Commerce, 5285 Port Royal Road, Springfield, VA 22161.

The findings of this report are not to be construed as an official Department of the Army position, unless so designated by other authorized documents.

The use of trade names or manufacturers' names in this report does not constitute indorsement of any commercial product.

REPORT DOCUMENTATION PAGE

Form Approved
OMB No. 0704-0188

1. AGENCY USE ONLY (Leave blank)	2. REPORT DATE	3. REPORT TYPE AND DATES COVERED
	January 1991	Final. May 89-Jun 90.

4. TITLE AND SUBTITLE

In-Flight Pressure Measurements on Several 155mm, M864 Base Burn Projectiles

5. FUNDING NUMBERS

1L162618AH80

6. AUTHOR(S)

Lyle D. Kaysar, John D. Kuzan, and David N. Vazquez

7. PERFORMING ORGANIZATION NAME(S) AND ADDRESS(ES)

8. PERFORMING ORGANIZATION REPORT NUMBER

9. SPONSORING/MONITORING AGENCY NAME(S) AND ADDRESS(ES)

Ballistic Research Laboratory
ATTN: SLCBR-DD-T
Aberdeen Proving Ground, MD 21005-5066

10. SPONSORING/MONITORING AGENCY REPORT NUMBER

BRL-MR-3888

11. SUPPLEMENTARY NOTES

12a. DISTRIBUTION/AVAILABILITY STATEMENT

Approved for public release; distribution is unlimited.

12b. DISTRIBUTION CODE

13. ABSTRACT *(Maximum 200 words)*

Four 155mm, M864 base burn projectiles were used to obtain in-flight measurements of pressure and temperature in the base region of the projectiles. The M864 uses the base burn concept of reducing base drag by injecting gas, generated by burning propellant, into the base area. Measurements of pressure and temperature were made in the chamber where the propellant was burned; pressure was measured in two locations on the base of the projectiles. Pressure was also measured near the nose of the projectiles, and yawsondes were used to measure projectile yaw. Data illustrate the increased base pressure that occurs while the propellant is burning, along with fluctuations in pressure due to projectile yawing motion.

14. SUBJECT TERMS

Projectiles
Base Flow
Solid Propellants
Injection

15. NUMBER OF PAGES

39

16. PRICE CODE

17. SECURITY CLASSIFICATION OF REPORT	18. SECURITY CLASSIFICATION OF THIS PAGE	19. SECURITY CLASSIFICATION OF ABSTRACT	20. LIMITATION OF ABSTRACT
UNCLASSIFIED	UNCLASSIFIED	UNCLASSIFIED	SAR

INTENTIONALLY LEFT BLANK.

Table of Contents

INTENTIONALLY LEFT BLANK.

List of Tables

INTENTIONALLY LEFT BLANK.

List of Figures

INTENTIONALLY LEFT BLANK.

I. Introduction

Of the three components of drag affecting a projectile in flight, base drag frequently accounts for one-half or more of the total drag. Base drag results from the low pressure associated with the wake and the region of separated flow behind the projectile. One method of reducing base drag is to increase the pressure in the base region through low speed mass injection into the wake. In the 155mm M864 base burn projectile, mass injection is in the form of gas generated from a burning solid propellant.

The solid propellant is housed in a propellant chamber located at the base of the projectile and the mass injection occurs through a hole in the chamber. The hole is not a nozzle, such as that found in a rocket-assisted projectile, so that the thrust resulting from the burning propellant is small.

Figure 1 shows a cross section of the propellant chamber; the assembly shown screws into the body of the M864 and becomes the projectile base. A propellant grain and two magnesium-teflon ignitors are shown installed in the assembly. The propellant grain used in the M864 resembles a doughnut that has been cut in half. The halves are separated by small spacers when the grains are installed in the projectile. Burning takes place on the cylindrical surface of the hole bored through the middle of the grain and on each of the four flat surfaces formed by cutting the grain in half. Thus, Figure 1 depicts two of the four flat surfaces; the ignitor housing resides in the cylindrical hole. The magnesium-teflon ignitors are designed to burn for two seconds to insure the propellant will reach a steady-state of burning.

Although the M864 projectile successfully uses a base burn system for extending its range, modeling techniques would be enhanced by in-flight measurements of temperature and pressure in the projectile propellant chamber and base region. The initial work performed to obtain such measurements on an in-flight projectile was presented in another report.[1]

The first in-flight measurement system was contained in the body of an M864 projectile; however, the test projectile weight and inertial properties did not match those of the M864. In that work, four measurements of pressure were made: two on the projectile base, one in the propellant chamber, and one on the projectile ogive. Temperature was measured in the propellant chamber and projectile yaw was measured with yawsondes.[2] The signals from the various measurements were telemetered back to a ground receiving station.

In the present work, four more projectiles were modified for in-flight measurements. In these tests, the center of mass, moments of inertia, and weight of the test projectiles closely matched the M864 projectile. Since this represents a continuation of earlier research, the reader is referred to the first report on the subject, Reference 1, for many of the details of the modifications to the shell.

[1] *Kayser, L.D., Kuzan, J.D., Vazquez, D.N., "Flight Testing for a Base-Burn Projectile System," BRL-MR-3830. Ballistic Research Laboratory Memorandum Report No. 3830, March 1990. AD No. A222562*

[2] *Mermagen, W.H., Clay, W.H., "The Design of a Second Generation Yawsonde," BRL-MR-2368, Ballistic Research Laboratory Memorandum Report No. 2368, April 1974 AD No. 780064*

Projectile Spin Rate (Hz): →			100	150	200
Gas	Density	Temp.	Pressure		
-	kg/m^3	K	Atm.		
air	1.204	293	.014	.030	.039
air	0.482	1810	.006	.012	.016
propellant	0.064	1810	-	.001	.002

Table 1. Effects of Projectile Spin on Base Corner Pressure Measurement

This work was supported by the Project Manager, Cannon Artillery Weapon Systems (PMCAWS) and the U.S. Army Research Development and Engineering Center (ARDEC), Picatinny Arsenal, New Jersey.

II. Experiment

The experimental apparatus consisted of M864 155mm base-burn projectiles instrumented to telemeter selected pressure, temperature, and projectile yawing motion measurements; a ground-based telemetry receiving station; a 155mm M199 Howitzer; a smear camera; and a Weibel radar system.

In order to make pressure measurements in the propellant chamber and at the projectile base, holes of 2.0 mm (5/64 inch) diameter were drilled in the walls of a standard M864 projectile base assembly, forming paths for pressure in one location to be sensed at another location. Figure 2 is a sketch of the base assembly and instrumentation canister, which also shows the paths for pressure at the orifices in the base area to be sensed by their respective pressure transducers.

The pressure transducers used in these experiments were purchased from the Kulite Corporation and were miniature, solid-state semiconductor strain-gage sensors with a four element bridge circuit. The transducers were rated for 25 psia full scale. The transducer sensitivity to acceleration was quoted to be typically 0.0005% of full scale per "g" perpendicular to the diaphragm and 0.0001% transverse to the diaphragm.

Figure 2 shows that there is a significant radial distance between the base corner pressure orifice and its pressure transducer. The gas in this system imparts a force on the transducer diaphragm. Centrifugal acceleration of the gas would make the measured pressure lower than the true pressure at the orifice. The size of the pressure difference would vary depending on the projectile spin rate and the density of the gas; this is shown in Table 1. It is not known if the propellant gas fills the pressure path, or if there is little or no flow at all inside the pressure path.

A hole was drilled through the transducer fixture and the front wall of the base assembly so that a thermocouple could be inserted into the propellant chamber. The thermo-

couple junction was located in a small gap between the igniter housing and the propellant grain and extended about 5 mm into the chamber. A tungsten- 5% rhenium– tungsten-26% rhenium was the type of thermocouple used. A slightly non-constant cold junction temperature of approximately 80° F inside the instrumentation canister was considered adequate for the much higher temperatures to be measured.

Circuit boards containing the electronics, depicted in Figure 2, and batteries for powering the electronics were mounted inside the instrumentation canister above the transducers. (Reference 1 explains many of the details involved in making in-flight pressure measurements and telemetering the results back to earth.) The main components of the electronics were a voltage regulator, voltage controlled oscillators, and a timer and switching device. The voltage regulator supplied power from the batteries to the pressure transducers and the thermocouple. The output voltages of the these sensors were amplified by a factor of approximately 30. Each voltage output was fed into a separate voltage controlled oscillator, operating at a unique center frequency. Here, voltage was converted to a frequency signal, then mixed and passed to the nose section of the projectile through a single conductor, ultimately to be broadcast back to the receiving station.

The timer and switching device shorted the output of the gages for 40 msec at 15 second intervals. The primary purpose in shorting the gages was to track any zero shift in the circuit.

The ogive of the projectile contained a pressure transducer which sensed the pressure on the forebody of the projectile. Solar sensors, mounted in the ogive flush to the exterior of the projectile, were used as the sensing device of a yawsonde that measured projectile yawing motion. The signals from the yawsonde and the forebody pressure transducer were amplified, converted to frequency signals, and then mixed with the signals from the base of the projectile. All of the mixed frequency signals were then used to modulate a transmitter carrier frequency of 250 Mhz. The signal broadcast from the projectile was received by antennas on the ground near the launch site and recorded on magnetic tape. The analog signals were later digitized and stored on a computer for data reduction and analysis.

An appendix to this report discusses the construction of the projectile instrumentation system and the problems encountered in its use.

III. Results and Discussion

The following tables show the projectile characteristics, the flight information and the success of measurements for all of the M864 projectiles that were fired. (Four of the projectiles are reported on in this work, Reference 1 gives the results of the first projectile that was fired.)

In Table 2, the ratio of the axial moment of inertia squared to the transverse moment of inertia is presented because that ratio appears in the gyroscopic stability factor, s_g:

$$s_g = \frac{I_x^2 p^2}{4 I_y \mu} \tag{1}$$

Projectile:	M864†	Flight 1	Flight 2	Flight 3	Flight 4	Flight 5	M864‡
Weight (kg):	46.7	38.5	46.4	46.2	46.9	46.9	45.4
CG (cm):	30.7	31.2	32.0	31.9	31.0	32.0	31.4
$I_x(kg \cdot m^2)$:	0.158	0.141	0.162	0.162	0.162	0.162	0.156
$I_y(kg \cdot m^2)$:	1.65	1.68	1.84	1.83	1.84	1.84	1.57
$I_x^2/I_y(kg \cdot m^2)$:	0.0151	0.0118	0.0143	0.0143	0.0142	0.0143	0.0155
†From an average of 25 shell.							
‡M864 with propellant grain removed; 10 shell average.							
The Center of Gravity (CG) is measured from the projectile base.							
I_x and I_y are the axial and transverse moments of inertia							

Table 2. Projectile Characteristics

Flight Number:	1	2	3	4	5
Date:	Aug '88	Jun '89	Jun '89	Nov '89	Nov '89
Launch Mach Number:	1.29	1.62	1.94	1.94	1.96
Elevation (mils):	850	850	1220	380	380
Sea Level Pressure (atm):	1.0075	1.0003	0.9996	0.9977	0.9959
Ground Temperature (C):	20.0	24.5	21.0	1.7	2.8
Propellant Temperature (C):	21	21	21	21	21

Table 3. Flight Information

Flight:	1	2	3	4	5
Chamber:	4 seconds on	to 22 seconds	Full Flight	Full Flight	5 seconds on
Base Corner:	Full Flight	Full Flight	Full Flight	No Data	10 seconds on
Base Flat:	Full Flight	Full Flight	55 seconds on	4-10 seconds	No Data
Nose Cone:	Full Flight	Full Flight	Full Flight	No Data	No Data
Temperature:	Full Flight	to 22 seconds	to 20 seconds	No Data	No Data
Yawsonde:	Little Data	Questionable	No Data	Full Flight	Full Flight

Table 4. Successful Measurements

where p is the axial angular speed (or spin rate) and μ is the static moment factor. The static moment factor is directly proportional to the static moment coefficient, C_{m_α} The table shows that inertial properities for the instrumented rounds slightly decreased the gyroscopic stability but the the center of gravity was farther from the base in the instrumented shell which decreases the static moment and increases the gyroscopic stability factor. Hence, the stability of the shell was not adversely affected.

Figure 3 shows the pressure in the propellant chamber, on the flat portion of the projectile base, and at the small recessed radius (base corner) of the projectile base for flight 2. Also shown is the ambient pressure at the altitude of the projectile (hereafter referred to as simply "ambient pressure"); this was obtained from weather balloons coupled with a projectile trajectory simulation computer program. Pressure in the figure is made dimensionless using the constant value of sea level atmospheric pressure. The data were low-pass filtered to remove fluctuations in the pressure resulting, primarily, from the projectile yawing and spinning motion. The chamber pressure measurement failed at approximately 22 seconds for unknown reasons. The predominant trend of the data is due to altitude changes that are indicated by a decreasing pressure on the up-leg portion of the trajectory and increasing pressure on the down-leg. The initial pressure rise, seen in the base flat and corner measurements, from zero to about 1.5 seconds occurred before the propellant grain reached steady state burning. At about two seconds, the decreasing atmospheric pressure dominates the trend of the data. At 18-19 seconds, the discontinuity in all three curves was caused by the transition from supersonic to subsonic projectile speed. The pressure reached a minimum at apogee, which occurred at about 32 seconds. Another discontinuity occurred at 35-36 seconds and coincides with propellant burnout. This discontinuity is not very obvious since the trend of the curves is dominated by the affect of altitude. Just prior to burnout, the the rate at which propellant gas is being generated is decaying which causes a decrease in the chamber and base pressures. When this pressure decrease is no longer evident, a discontinuity occurs and burnout is assumed to be complete. The discontinuity at burnout will be more apparent in subsequent figures where the base pressures are made dimensionless with local ambient (static) pressure. Propellant burnout allows a pressure gradient across the base of the projectile to develop, and this results in a difference between the base flat and corner pressures after 35 seconds. In a recirculating base flow, a local stagnation region would be expected near the center of the projectile base along with a higher pressure. This higher pressure near the center suggests a pressure gradient that has the qualitative trend of the experimental data that show a lower pressure at the base corner. The gradient was extinguished by the propellant gas before this time. The chamber pressure approached the ambient pressure as the projectile slowed to a Mach number of one, and then was above ambient once the projectile speed was subsonic. This is shown more clearly in the next figure.

Figure 4 shows the same three pressure measurements normalized with the ambient (local static) pressure. The predominant trends of the data are now due to the propellant gas and the aerodynamics of projectile base flow rather than altitude changes over the trajectory. All three pressures ratios increased as the projectile slowed to sonic speed. After the sharp discontinuity resulting from the transition from supersonic to subsonic speed, the base corner and base flat pressures were nearly constant at approximately 97% of the ambient pressure. At 28 to 30 seconds, the base pressures start to decrease and

a discontinuity, indicating propellant burnout, occurs at about 35 seconds. The pressure gradient across the base that appeared after propellant burnout is more distinct in this figure. This is consistent with the results of flight 1. Figure 5 is an expanded view of the previous figure. This shows the increase in pressure to the steady state propellant burn rate (from zero to 1.5 seconds) more clearly.

After the ground tests and flight 1, Danberg[3] developed a model for in-flight propellant performance. Using that model, propellant chamber and base pressures can be computed for the launch conditions of flights 1 through 5 described in this report. Figure 6 shows the measured and computed chamber and base pressures which were made dimensionless with the ambient pressure, *for flight 1.* The computational base pressure predicted using Danberg's model is an averaged base pressure and pressure gradients on the base are not predicted. The details of the computed pressures compare reasonably well to the measured pressures although some discrepancies will be noted. Because of a pyrotechnic delay, the chamber pressure was not sensed until about 4 seconds into the flight. At about 8 seconds, the pressure discontinuity is an indication of transition from supersonic to subsonic speed. The computed chamber pressure appears to be equal in magnitude to the measured pressure while the propellant was burning and the projectile speed was subsonic. Propellant burnout was computed to occur about 2 seconds after the measurements suggest it occurs. Burnout is assumed to occur where the pressure curves exhibit an abrupt change in direction which is at about 35 seconds for the measured pressures and at about 37 seconds for the computed pressures. Computed base flat pressures are about 2% lower when the projectile speed is subsonic, whether or not the propellant is burning. In the early part of the flight, at supersonic speeds, both the base flat and chamber pressures are on the order of 6-10% lower than the measured pressure; the propellant is burning at that time. The effect of the magnesium-teflon ignitors is to form a small spike in both the measured and computed pressures curves at 2 seconds.

Figure 7 shows the measured in-flight and computed pressures, made dimensionless with the ambient pressure, for flight 2. The computed pressures are lower than the measured pressures until about 10 seconds into the flight. At about 17 seconds, the abrupt rise in measured and computed pressures is caused by transition from supersonic to subsonic flow. At about 21 seconds, the chamber pressure measurement is seen to have failed and the computed pressure at that time is somewhat higher. The sudden drop in pressures around 35-38 seconds indicates burnout of the propellant. The predicted pressures are again seen to be lower than measured values in the early part of the flight but during the latter part of the burn phase, 18-37 seconds, predicted values are higher. The measured base pressures indicated burnout at about 35 to 37 seconds and the predicted burnout time is 38 seconds or about 2 seconds later.

Figure 8 depicts pressures for flight 3 and is similar to Figure 3. The base flat pressure measurement was erratic until approximately 55 seconds into the flight for unknown reasons. Again, the predominant trend of the data is due to altitude changes. Two transitions

[3] Danberg, J. E., "Analysis of the Flight Performance of the 155 MM Base Burn Projectile," BRL-TR-3083, Ballistic Research Laboratory Technical Report No. 3083, April 1990, AD No. ADA222624

through the sonic speed are seen in the base corner pressure measurements: one at about 23 seconds (supersonic to subsonic) and another at about 78 seconds (subsonic to supersonic as the projectile accelerates on the down-leg of the trajectory). The discontinuity at 78 seconds can also be seen in the chamber and base flat pressures.

At approximately 20 seconds there is a large increase in the chamber pressure that masks the discontinuity associated with the supersonic to subsonic transition. Initially it was thought that this could be a manifestation of a choked-flow at the exit of the propellant chamber. A brief analysis of the required conditions indicates that choking probably did not occur. Choked-flow occurs when the exit speed of the gas reaches the sonic speed. In air this would happen when the chamber pressure is 1.89 times the value of the exit pressure. The ratio of specific heats for the propellant gas is not known but for a wide range of specific heat ratios, chamber pressure would have to be 1.8 to 1.9 times the exit pressure. If the base corner pressure is assumed to be equal to the exit pressure (based on other data, this is a reasonable assumption), then the chamber pressure is about 1.4 times the exit pressure when the chamber pressure begins to increase at 19 seconds into the flight. At 20 seconds, the ratio reaches a maximum value of 1.58 which is still too low to indicate a choked flow. It is believed that the base corner pressure is much lower than it should be because base pressure is expected to be fairly close to the ambient pressure in the subsonic portion of the flight (22 to 78 seconds). If the measured base corner pressure is too low, the above ratios of 1.4 and 1.58 would be even smaller and make the possibility of choked flow even more remote. The reason for the sudden increase in pressure is not known but it could be speculated that a flaw or cavity within the grain could cause an increased burning rate and hence an increased pressure.

The large spike in the chamber pressure curve at 18 seconds, and shortly before the sudden pressure increase could be from voids in the propellant grain. These spikes have been seen before in both ground and flight tests – figure 6 shows a similar spike at 23 seconds.

Because of the high altitude and lower burn rates, the time of propellant burnout is not as easily detected as it was in the previous flight. Propellant burnout may be indicated around 40 seconds where the chamber pressure and base corner pressure curves diverge somewhat. Between 30 and 40 seconds, there is a near constant difference between the two pressures, and this is consistent with previous flight data in the subsonic regime. The difference then begins to grow after 40 seconds. The interpretation is that the propellant gas extinguishes the pressure gradient across the base of the projectile, so that when the propellant burns out the base flat and base corner pressure measurements no longer coincide. Also, when the propellant burns out, the chamber pressure measurement is very close to the base flat measurement, although before this time it is significantly greater than the base flat pressure. It is possible that the diverging pressures at 40 seconds indicate that burnout is approaching but not yet complete. The corner pressure shows a discontinuity at 70 seconds which is somewhat characteristic of burnout. A burn time of 70 seconds may be possible but seems unlikely.

Although the ambient pressure is shown on this figure, it may not be too accurate. because of the high quadrant elevation at launch, the trajectory simulation may not have given accurate altitude results. For this reason, the pressures made dimensionless with

ambient pressure shown in Figure 9 may show some distortion. For example, the chamber pressure ratio is not expected to be less than unity as seen in the time period of 30 to 55 seconds. The base corner pressure appears much to low after the early part of the flight; a drift in the circuit voltage is suspected after 10 seconds. Nevertheless, the trend of the data suggests that the pressure measurement still functioned, since the sonic speed discontinuity appears correct at about 22 seconds and again at 78 seconds. The time of burnout for this flight, as stated above, is not easily detected. The chamber pressure seems to show a change in trend at 40 seconds but no corresponding change is seen in base-corner curve. At 45-46 seconds both the chamber and base-corner curves show a change in trend which is consistent with propellant burnout. Discontinuities in all three curves are seen at 70 seconds which could indicate the time of burnout. A burn time of 70 seconds may not be out of the question since Danberg[4] observed burn times of more than 80 seconds for an M864 flight. The M864 was launched with an M203 charge at 1150 mils and a propellant temperature of -20C.

After the base flat pressure started functioning, it followed the trend of the chamber pressure but relative to the chamber pressure the overall level seems about 5% too low. The data in this figure were not filtered; this gives an impression of the fluctuations in the pressure signal that result from projectile spin and yaw, and noise.

A comparison of flight 3 to Danberg's model is shown in Figure 10 and in this figure, the measured pressure has been low-pass filtered. The low level of measured chamber pressure from 30-60 seconds seems unrealistic and the pressure on the base flat also seems too low from 50-60 seconds. Firing tables data that suggests that the trajectory simulation may have predicted an apogee about 8 percent too low. A lower ambient pressure at higher altitude would have raised the dimensionless chamber pressure at apogee and improved agreement with Danberg's prediction. Burnout is computed to be at 49 seconds, and while the time determined from measurements seems to be 40, 45-46, or 70 seconds, the 45-46 second value seems more convincing. Once again, the computed pressures seem to be lower in the early stages of flight.

Figure 11 shows the nose cone pressures for flights 1 through 3, as well as the surface pressure on a sharp nosed cone from wind tunnel data. The pressure is shown versus Mach number. In all the flight data, the discontinuity that is caused by the transition from supersonic to subsonic speed occurs in advance of the time the discontinuity is found on the base region pressure curves. This suggests that the discontinuity is associated with a shock that is attached to the nose at high Mach numbers and detaches at about a Mach number of 1.05. When the shock detaches, there is an increase in the pressure on the surface of the nose cone. It is disturbing that the pressures are not equal for each of the flights. No computations were made for the nose cone pressures but the results for flight No.1 appear to be the most accurate. The discrepancies appear to be primarily a zero shift in the data signals. Such a shift could have occurred in the transducer or by a frequency shift in the VCO. High pressure gun gases could not have been a factor at the forward location on the projectile.

[4]Danberg, J. E., Private Communication

The projectiles in flights 4 and 5 were launched at the same quadrant elevation and with the same type propelling charge; the difference between the two flights was that the projectile in flight 5 did not have a propellant grain. Thus, flight 5 was to serve as a tare experiment. Both of the trajectories are quite low for artillery projectiles, so the ambient pressure at apogee was only 20% lower than the ground pressure.

Figure 12 depicts pressures for flight 4 which are made dimensionless with sea level atmospheric pressure similar to those of Figure 3. The base flat pressure seemed reliable between 4 and 10 seconds only, and the base corner pressure failed. In ground tests, it was found that the propellant grain had a progressive burn and that the burn became more progressive as the spin rate increased. In flight 4 the spin rate was relatively high, and the change in pressure due to altitude was not that substantial, so it is expected that the progressive burn nature of the propellant might dominate the pressure curve, as it appears to do after about two seconds into the flight. The first two seconds of the flight show complex pressure variations due to the burning of the magnesium-teflon igniters and the propellant ignition process. At 18 seconds, there is a sudden pressure rise similar to that seen in flight 3. The phenomenon which causes this sudden rise is not understood but is not believed to be a choked flow. Near 27 seconds, the propellant burns out and the pressure drops quickly. At about 30 seconds, the projectile has slowed to the sonic speed and there is a discontinuity in the pressure curve. Previous flights have shown that the pressure loss in the chamber due to the propellant burnout is approximately the same as the pressure increase due to the transition through sonic speed, and this appears to occur in flight 4 as well. The increase in pressure is enhanced by the return to higher ambient pressure.

The small segment of base flat pressure reflects the increase in pressure that was due to the combination of faster propellant burn rate and small ambient pressure change.

Figure 13 shows the chamber and base flat pressures, both measured and computed, made dimensionless with the ambient pressure. Here the progressive burn of the propellant is somewhat more apparent in the measured pressure. It is also clear that the decrease in pressure from burnout is nearly the same as the increase in pressure from the transition to subsonic speed. The chamber pressure measurement indicates burnout at 28 seconds compared to the computed burnout time of about 33 seconds. These burnout times are in sharp contrast to those of flight 3 which indicate burnout times of 45-46 seconds (experiment) and 49 second (computation). The longer burn time for flight 3 demonstrates the effect of the lower pressure (high altitude) environment which decreases the propellant burning rate. The computed pressures for the early part of the flight are lower than measured values and the differences are similar to those of flights 1, 2, & 3.

For flights 4 and 5, two independent measurements of chamber pressure were made. Figure 14 shows a comparison of these two measurements for flight No. 4. The 22 kHz (VCO frequency) channel was not functioning properly until about 18 seconds into the flight. After 18 seconds, the 22 kHz data followed the trends of th 94 kHz data but was consistently lower by a few percent. The 94 kHz data are presented in Figure 12 and Figure 13.

Flight:	1	2	3	4
Average Spin Rate While Burning (rev. per sec):	130	162	195	189
Average Ambient Pressure (std. atm.):	0.732	0.631	0.430	0.825
Propellant Burn Time (sec):	**35**	**35**	**45**	**28**
Ground Test Spin Rate (rev. per sec):	142	176	199	253
Ground Test Burn Time (sec):	29	27	26	24
Danberg Propellant Burn Time (sec)	37	38	49	33

Table 5. Average Spin Rate, Average Ambient Pressure and Burn Time for All Flights

Figure 15 shows the 94 kHz chamber and base corner pressures for flight 5, which carried an inert propellant grain. Figure 16 shows the pressures made dimensionless with the ambient pressure and the computed base pressure. Comparison of the measured base corner pressure with the predicted base pressure, Figure 16, shows consistent behavior and both curves show the transonic pressure rise. Agreement in the subsonic portion of the flight is quite good. Figure 17 shows a comparison of the 22 kHz and 94 kHz chamber pressures. The base corner and chamber pressures, as seen from Figure 15 and Figure 17, show the same trends after 20 seconds into the flight but the chamber pressures are much too low. The base corner measurement seems to be the only reasonably reliable pressure measurement for thi. .light.

Table 5 shows the variation of propellant burn time with the ambient pressure and the spin rate of the projectile. It also shows some of the results of ground tests at sea level atmospheric pressure. Since the propellant burn rate varies with both ambient pressure (see Miller and Holmes[5]) and spin rate, the results of the flight tests do not match exactly the ground tests. For example, at about 199 revolutions per second, the ground test propellant burn time was 26 seconds, while in flight at a average spin rate only 4 revolutions per second slower the burn time was 45 seconds. The difference was in the ambient pressure; flight 3 went to very high altitude. If the ground test burn times were adjusted for the lower pressures, high altitude conditions, according to the findings of Miller and Holmes, longer burn times would result. The longer burn times determined from the flight cases are therefore consistent with the ground test results and with the experiments of Miller and Holmes.

Table 4 shows that a limited amount of temperature data were obtained for flights 2-5 and no temperature data are presented. For flight 1, the temperatures were obtained for the entire flight, and although measurements were erratic and are not believed be accurate, they do provide some boundaries on gas temperature. Also, the thermocouple responded to a significant pressure 'burst' and gave a clear indication of propellant burnout which illustrates the potential value of the thermocouple in detecting the certain events.

[5] *Miller, M.S., and Holmes, H.E., "An Experimental Determination of Subatmospheric Burning Rates and Critical Diameters for AP/HTPB Propellant," Ballistic Research Laboratory Memorandum Report No. 3719, December 1988 AD No AD201109*

Gun pressures and projectile accelerations were: approximately 12000 psi and 3800 g for the first flight, 24000 psi and 6900 g for the second flight, and 32000 psi and 8100 g for flights 3, 4, and 5. The best results were obtained from the first flight but the quality of data seemed to deteriorate with the increasing severity of the launch conditions. A discussion of the data quality and failures is provided in the appendix along with some speculations about the problems that were encountered.

IV. Conclusions

1. The in-flight measurements clearly show the effects of various parameters such as; Mach number, altitude, gas injection, projectile spin, transition from supersonic to subsonic flow, and propellant burn time.

2. The chamber temperature measurements show erratic behavior and generally do not reflect the accurate values of gas temperature. A thermocouple, with a more rugged design which would function for the entire flight and respond to certain events, could be of substantial value even if accurate measurements are not obtained.

3. Comparison of measurements to predicted quantities shows that the model developed by Danberg provides a good description of the events that occur during the base burn process. The most significant difference between the computation and experiment is that predicted pressures are consistently lower during the early segment of the burn phase

4. Ground tests showing the combined effects of spin rate and ambient pressure (altitude) would provide a valuable input to the predictive capability.

5. The quality of signals decreases and the number of failures increases as the severity of the launch conditions increase.

6. The success of the first flight provided the impetus for instrumenting and testing projectiles for flights 2-5.

7. Due to the number of problems encountered in flights 3-5, further development and assessment of techniques are needed before additional flights with such complex instrumentation are carried out.

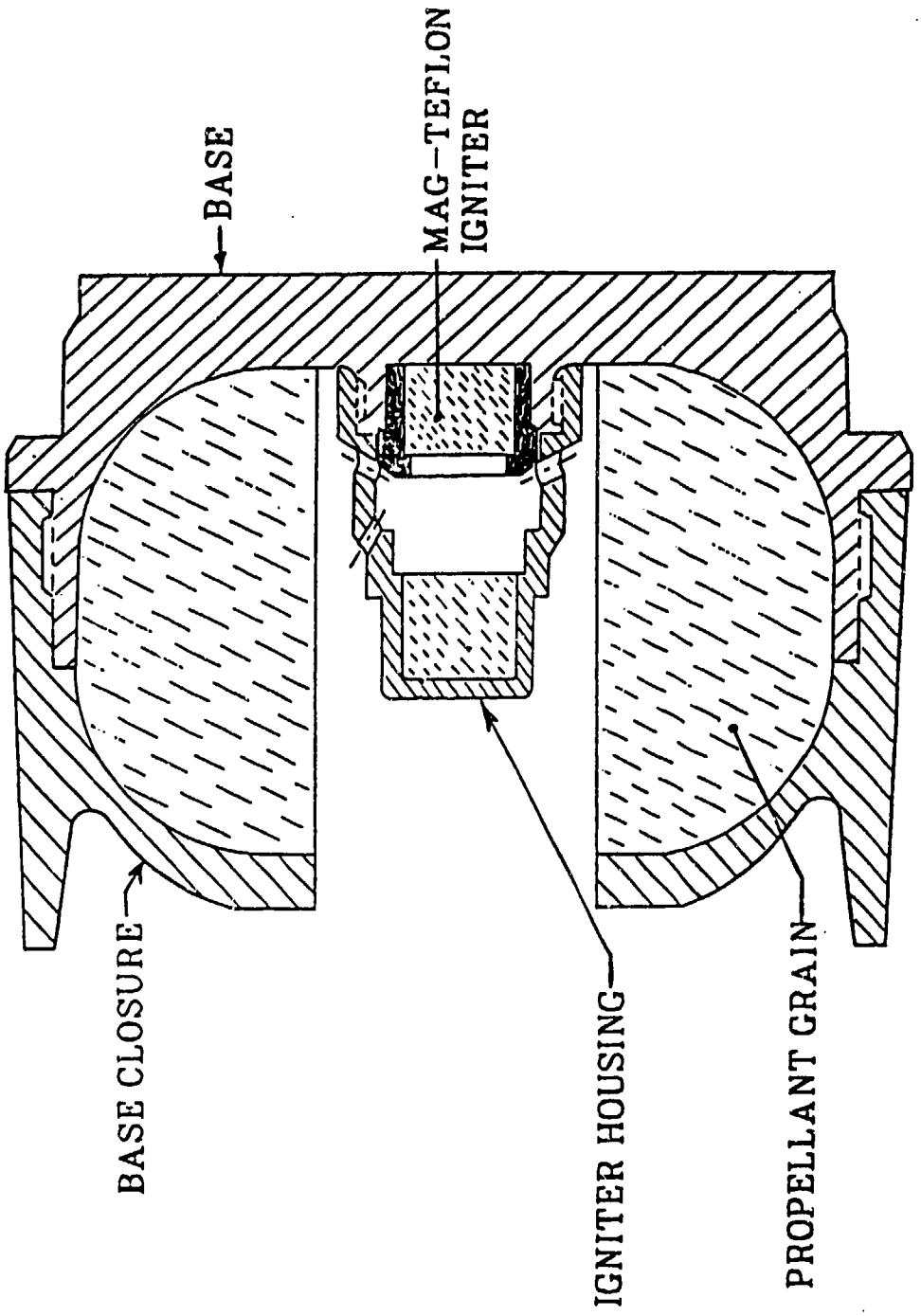

Figure 1: M864 Projectile Base Burn System

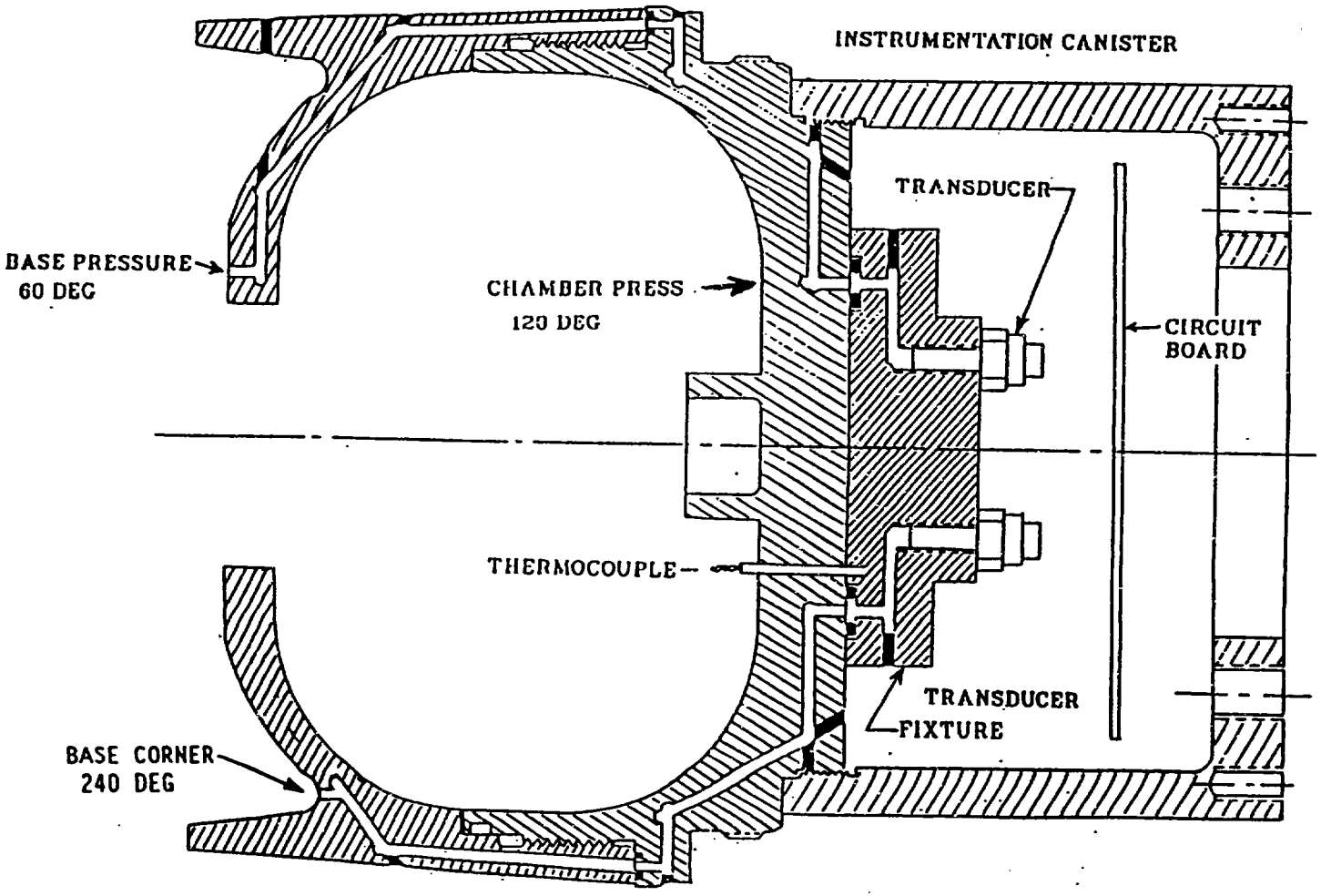

Figure 2: Modified M864 Projectile Base

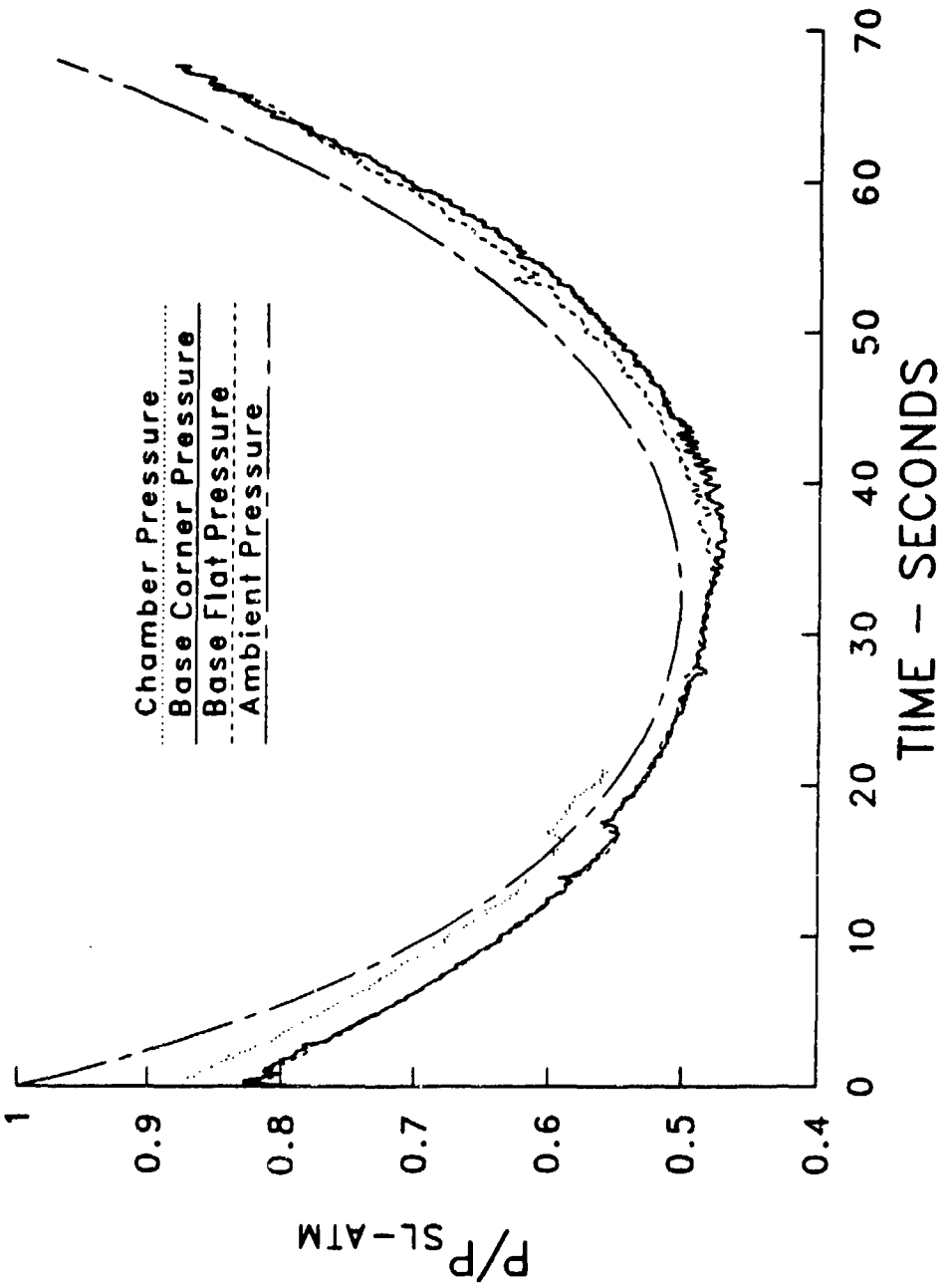

Figure 3: Flight 2—Base Corner, Flat; Chamber Pressures

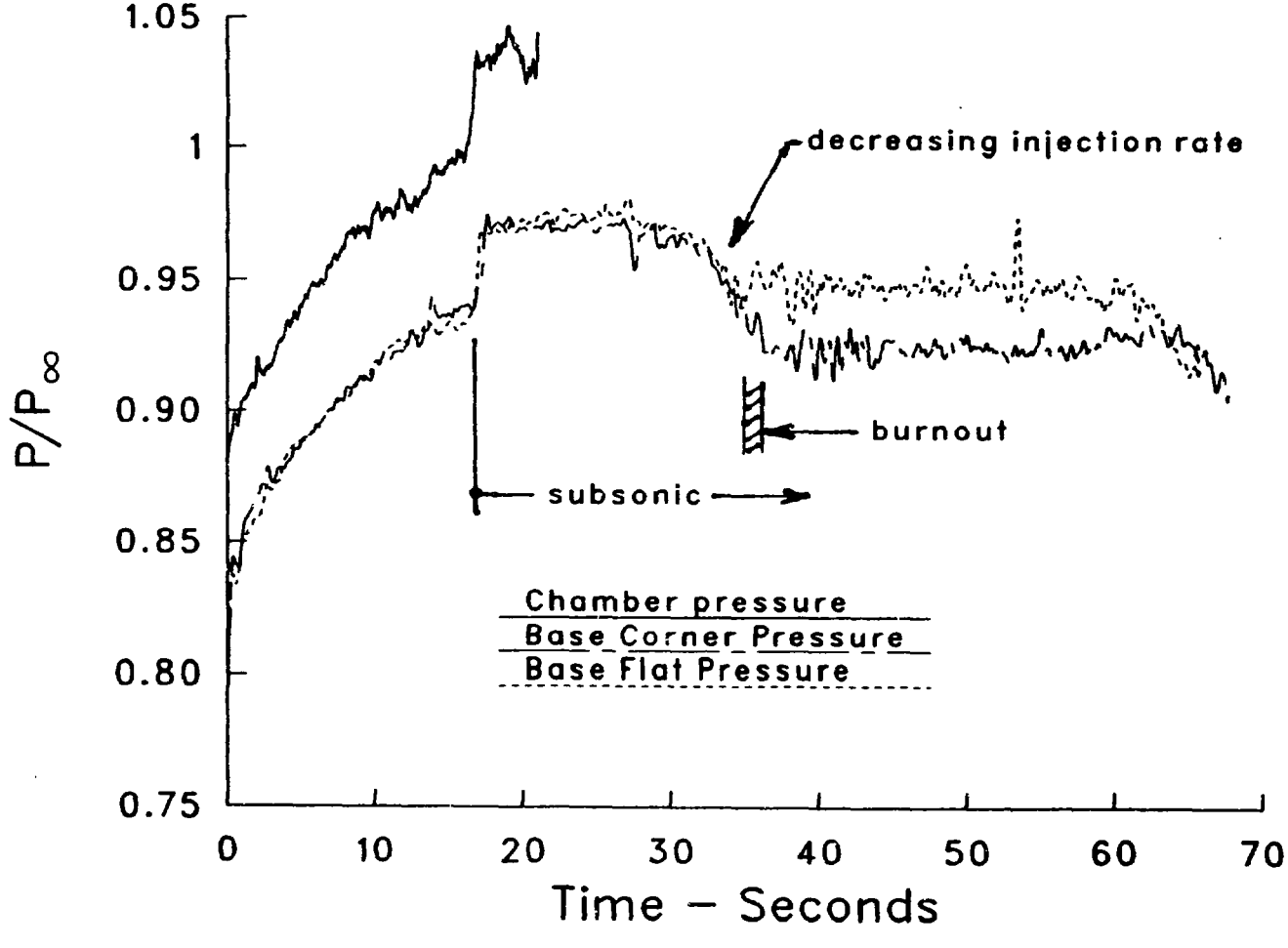

Figure 4: Flight 2—Base Corner, Flat; Chamber Pressures—Normalized

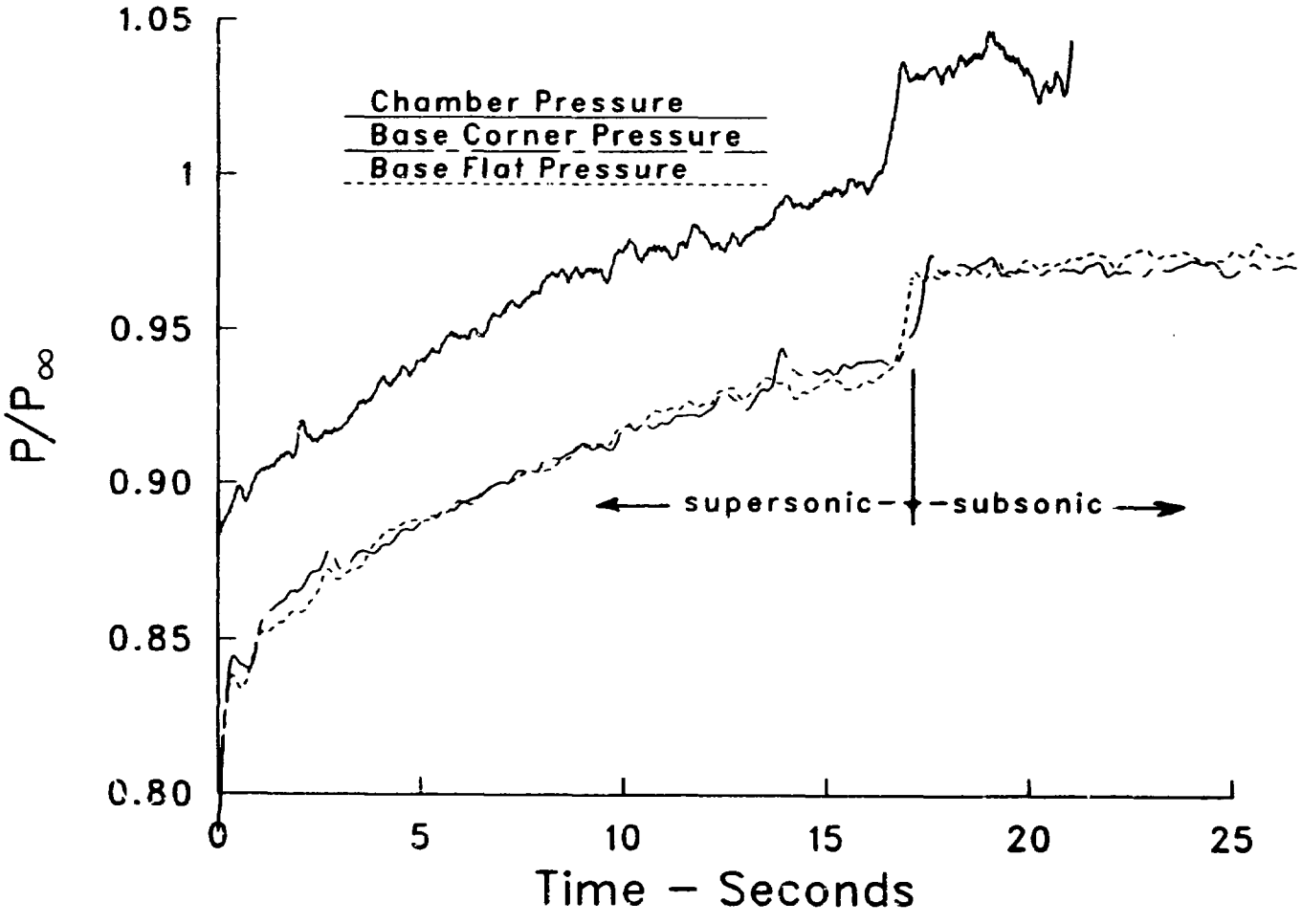

Figure 5: Flight 2—Base Corner, Flat; Chamber Pressures—Expanded

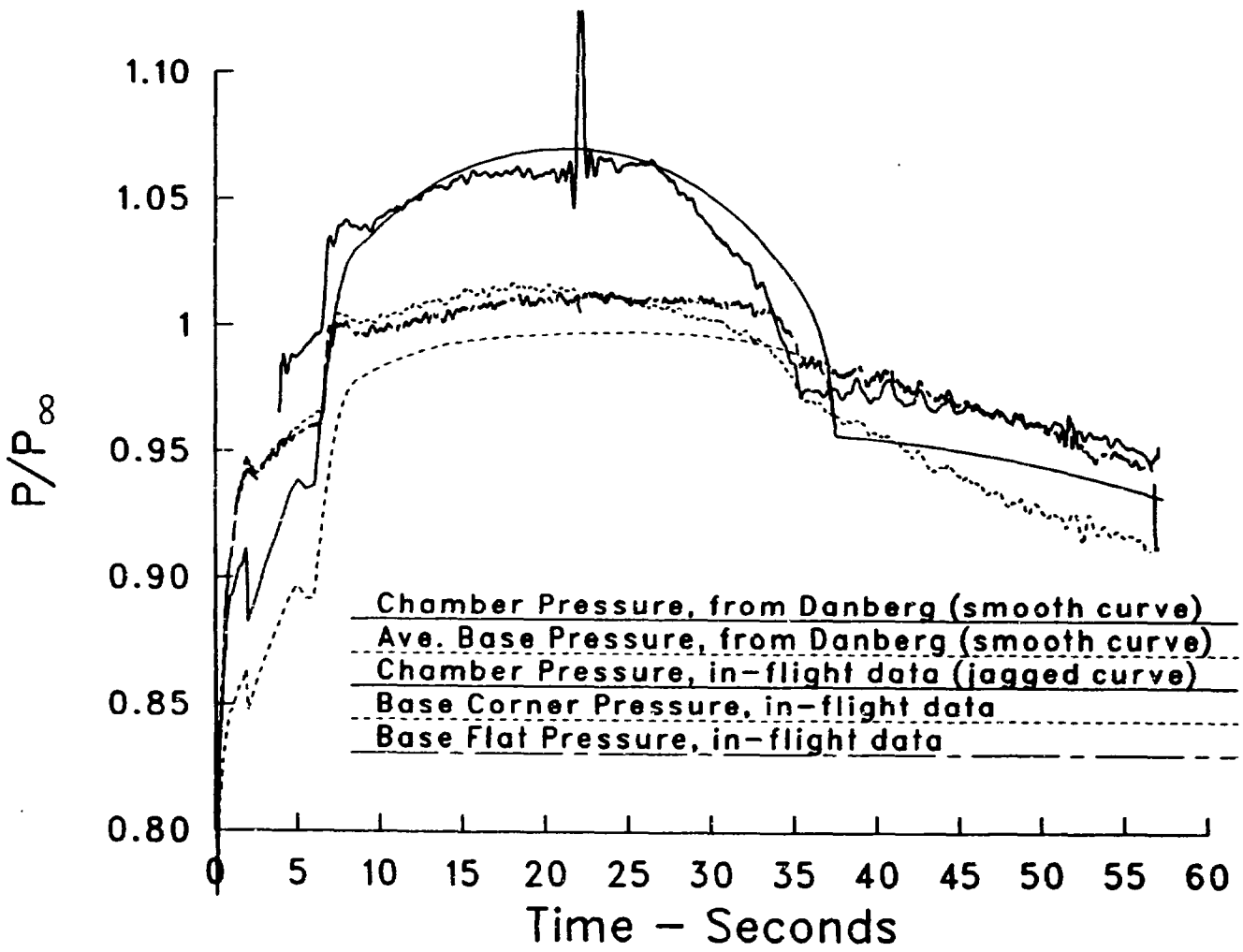

Figure 6: Flight 1—Base Corner, Flat; Chamber Pressures, Measured and Computed

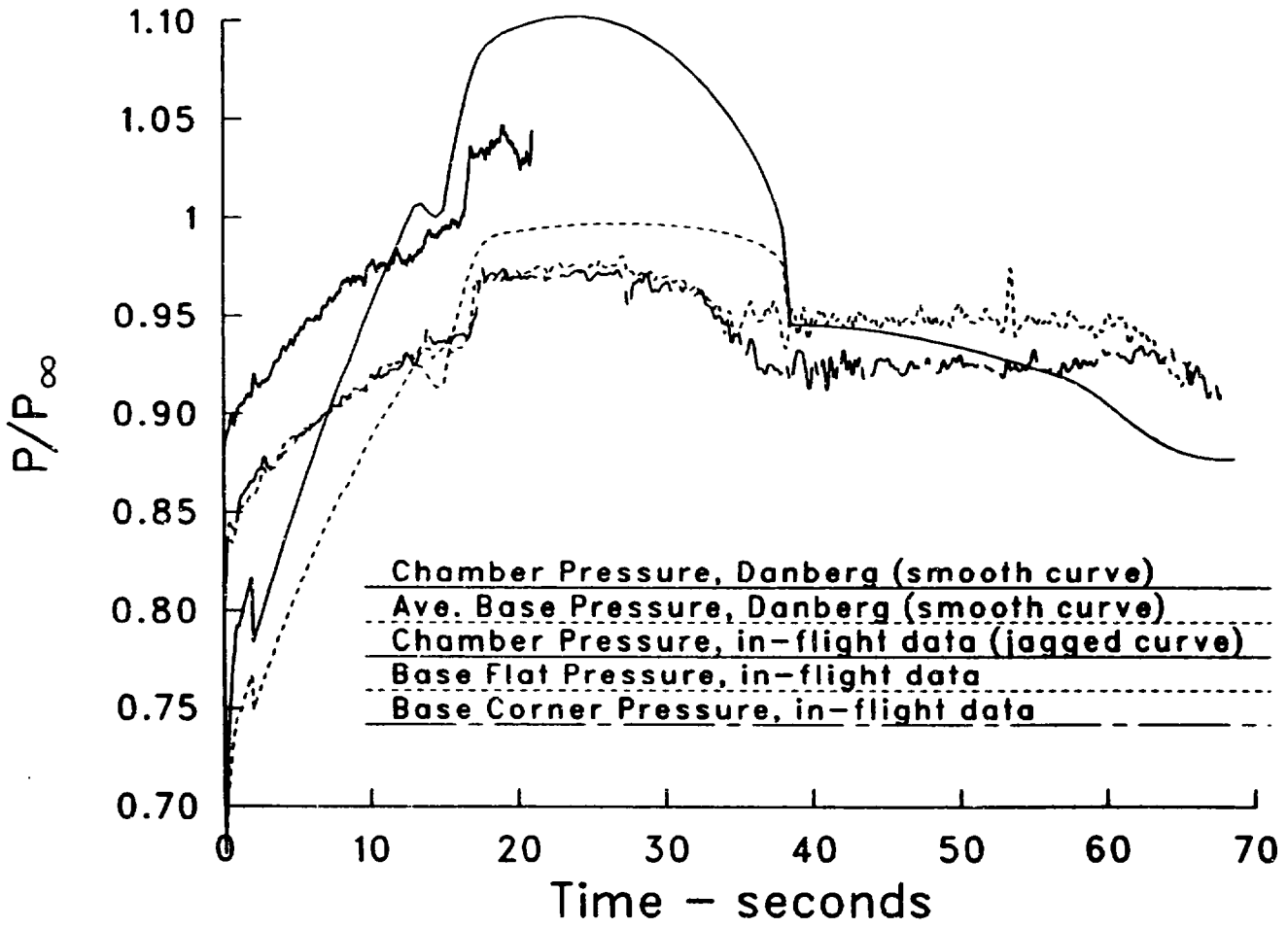

Figure 7: Flight 2—Base Corner, Flat; Chamber Pressures, Measured and Computed

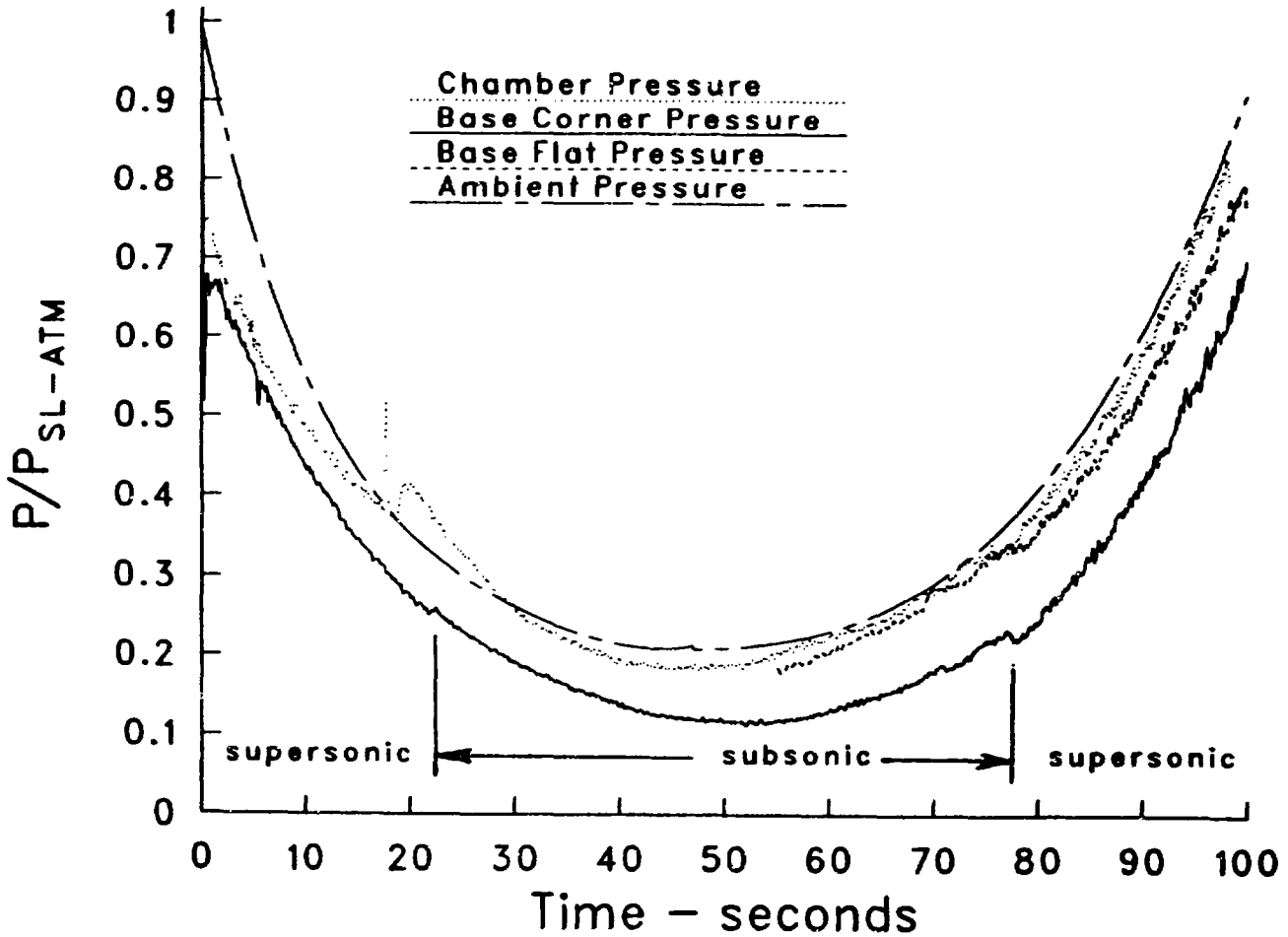

Figure 8: Flight 3—Base Corner, Flat; Chamber Pressures

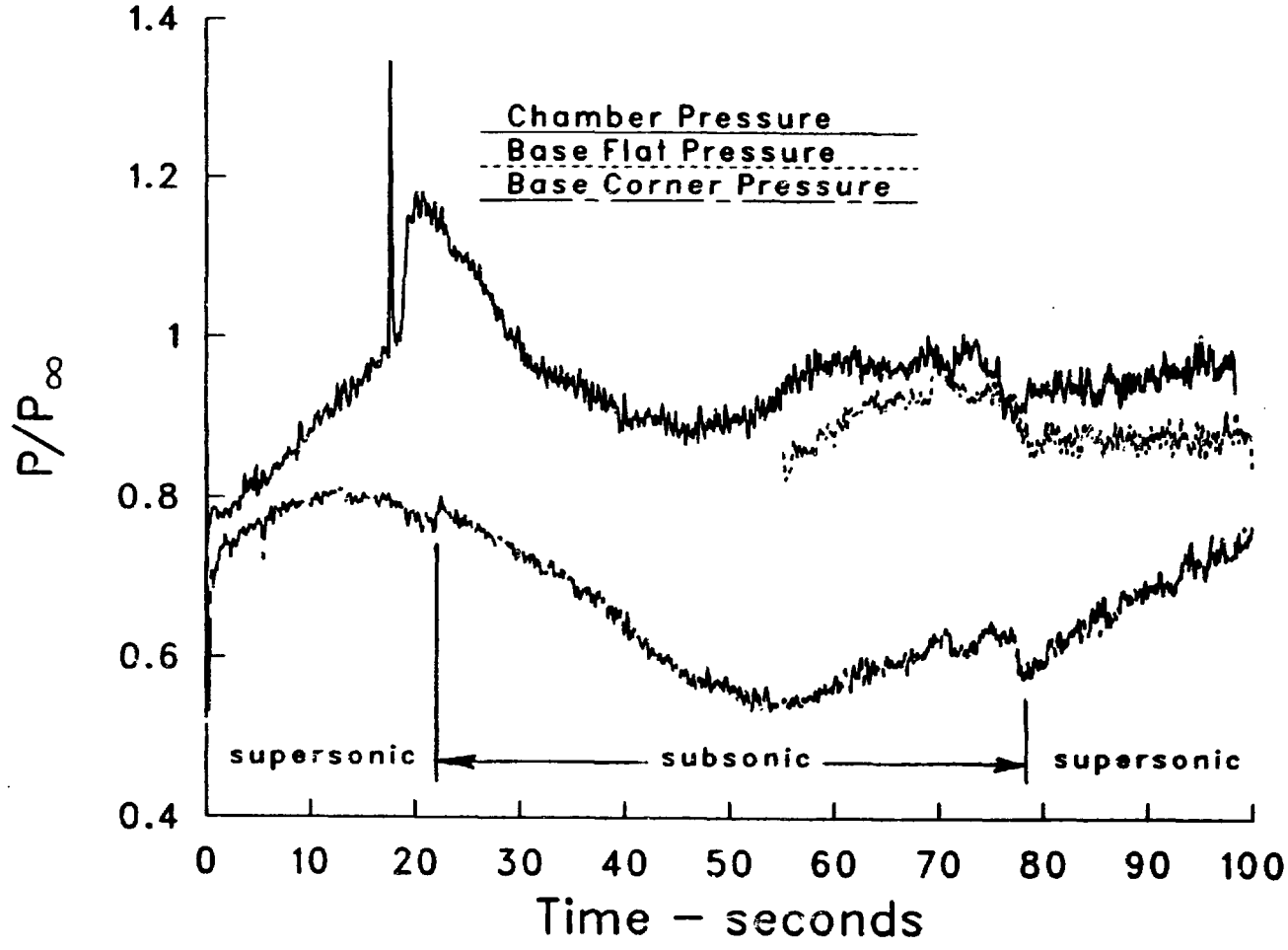

Figure 9: Flight 3—Base Corner, Flat; Chamber Pressures—Normalized

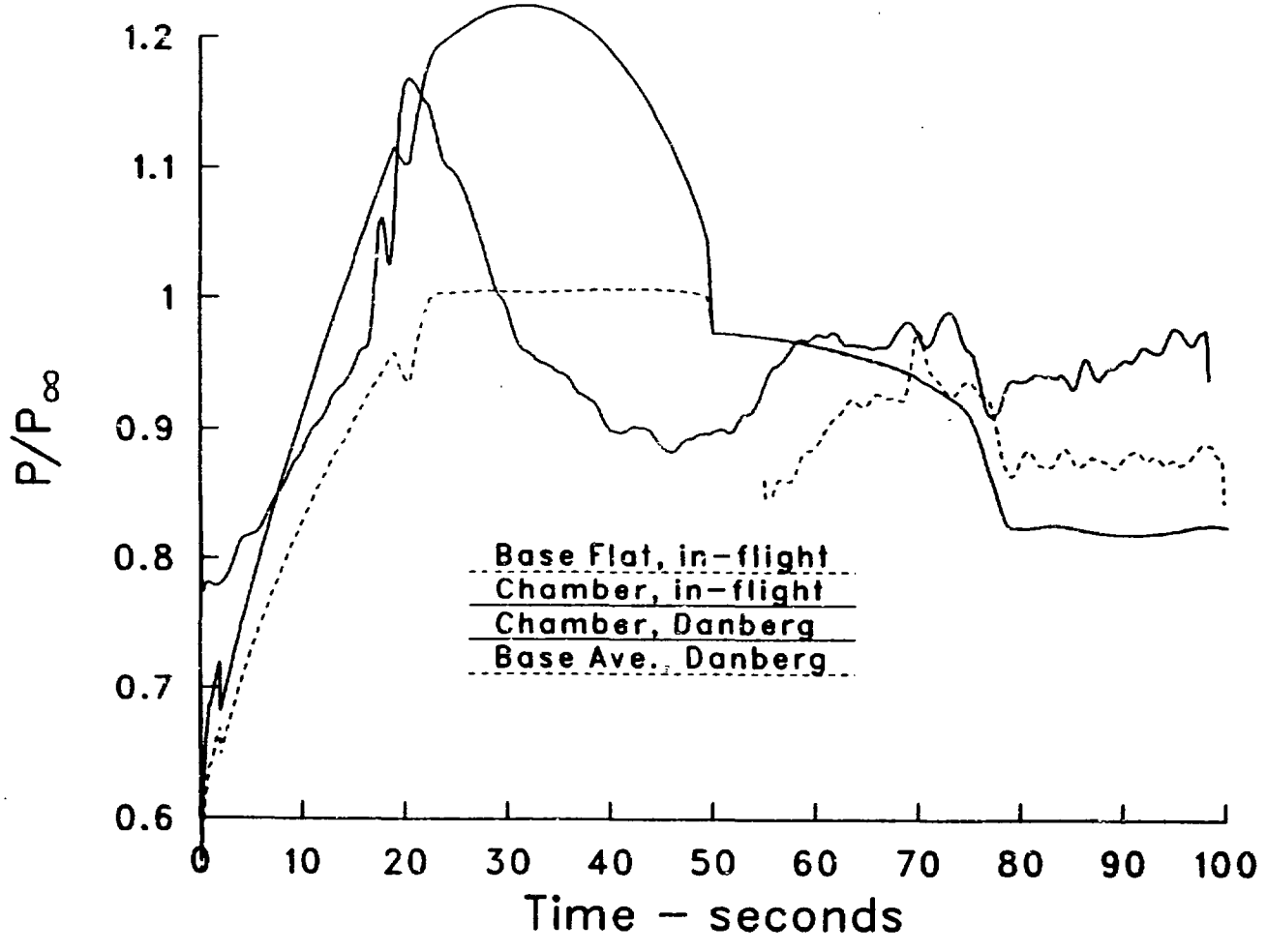

Figure 10: Flight 3—Base Corner, Flat; Chamber Pressures, Measured and Computed

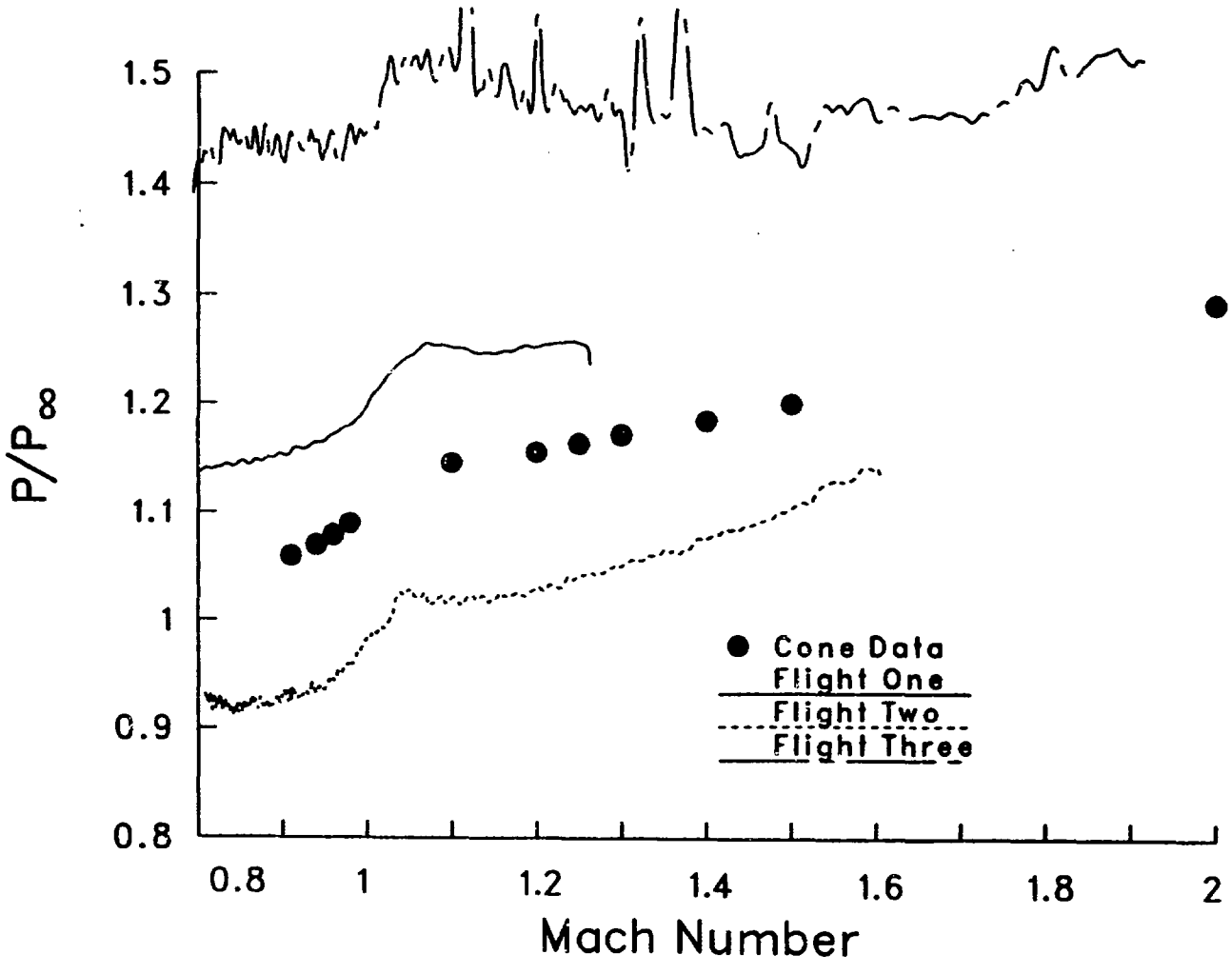

Figure 11: Flights 1 through 3—Nose Cone Pressures

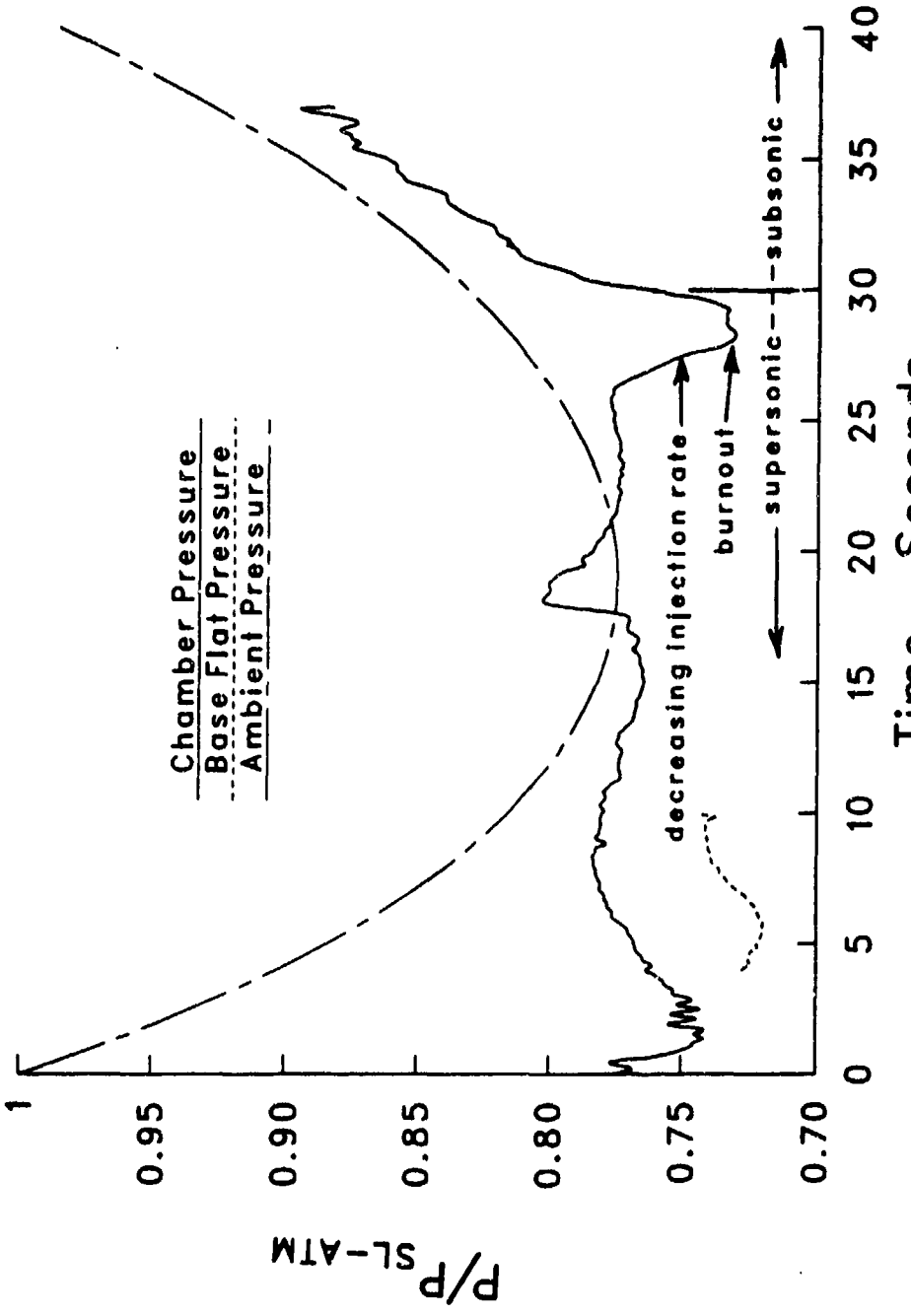

Figure 12: Flight 4—Base Flat, Chamber Pressures

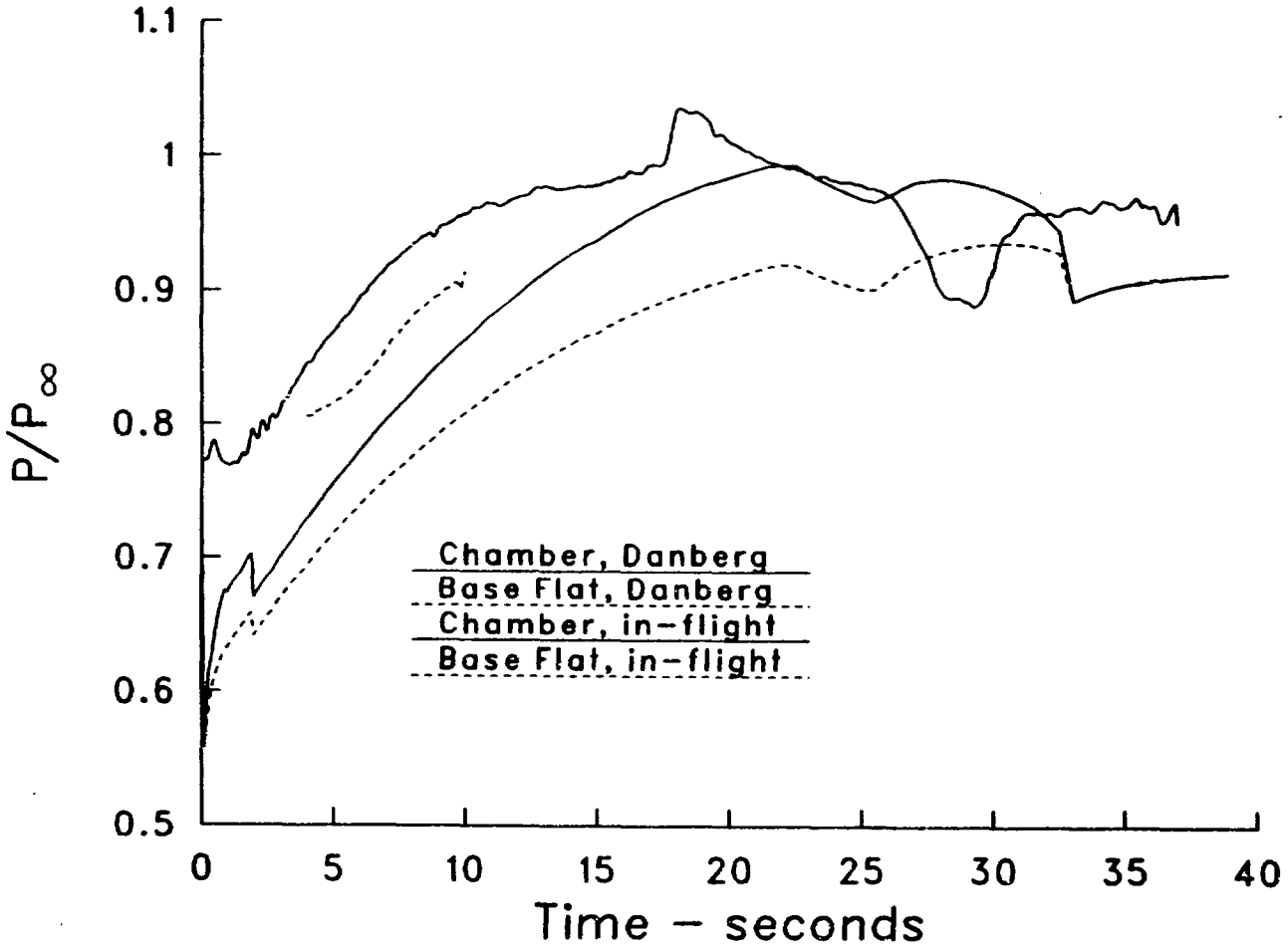

Figure 13: Flight 4—Base Flat, Chamber Pressures, Measured and Computed

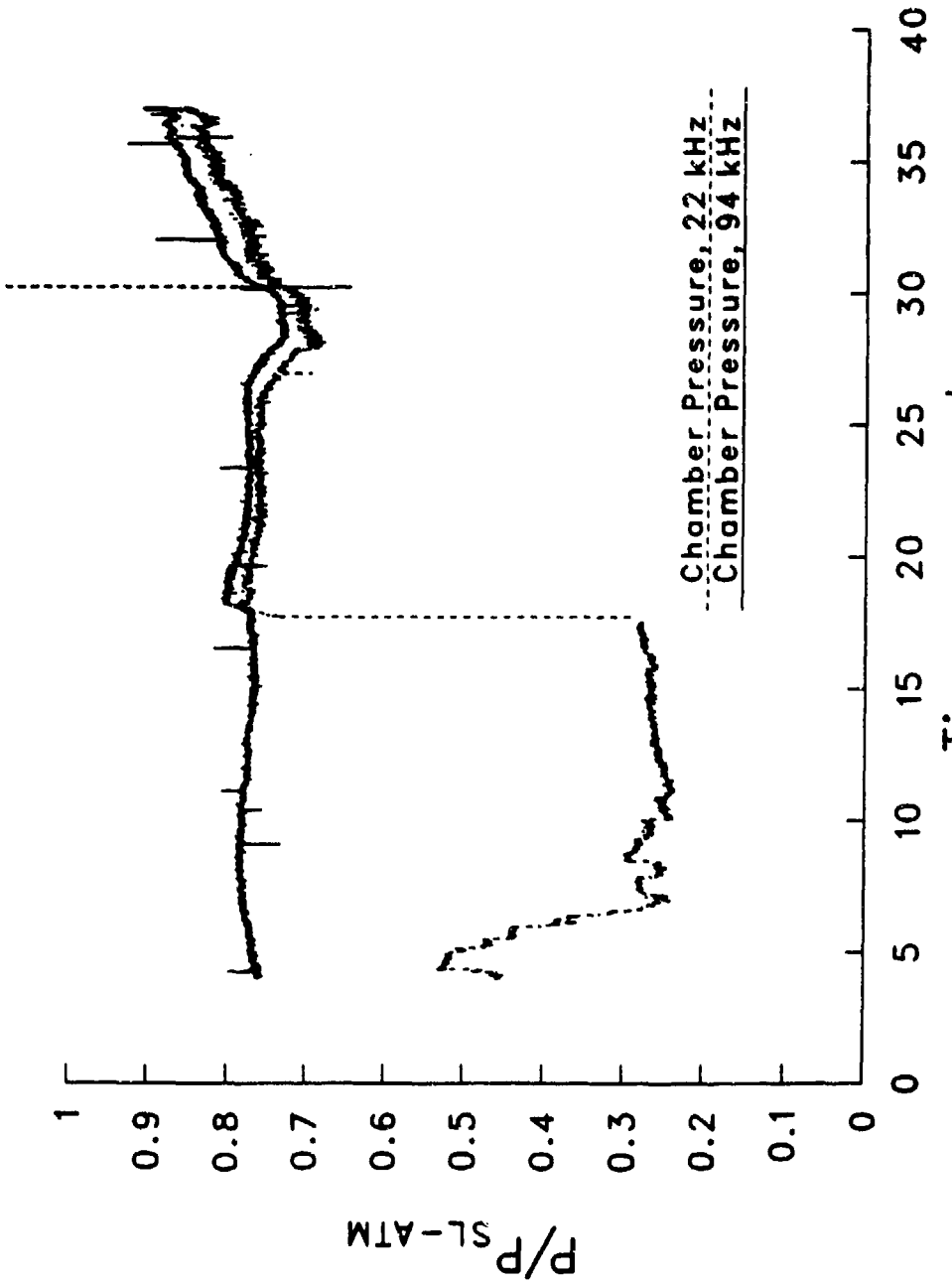

Figure 14: Flight 4—22 kHz and 94 kHz Chamber Pressures

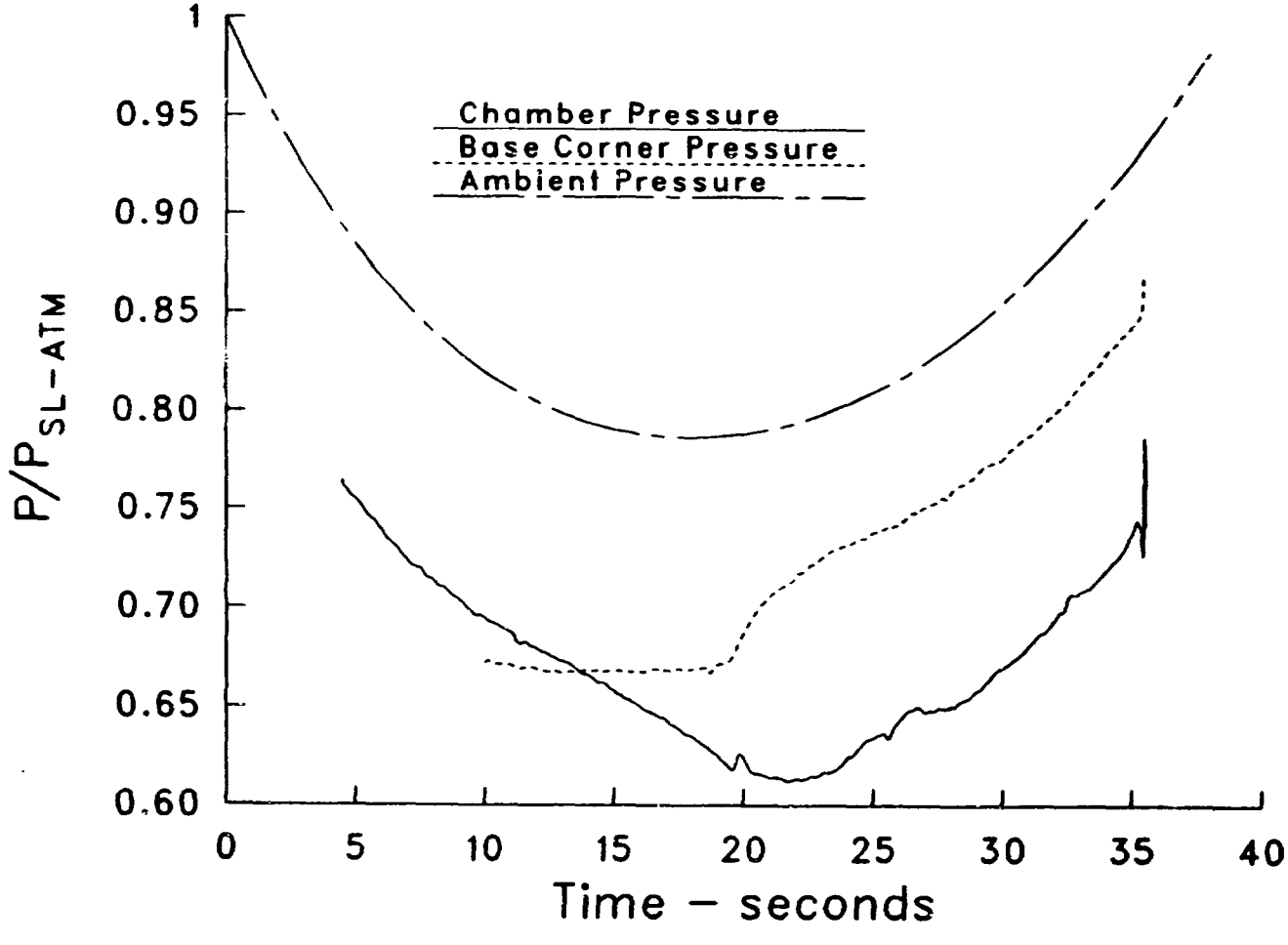

Figure 15: Flight 5—Base Corner, Chamber Pressures

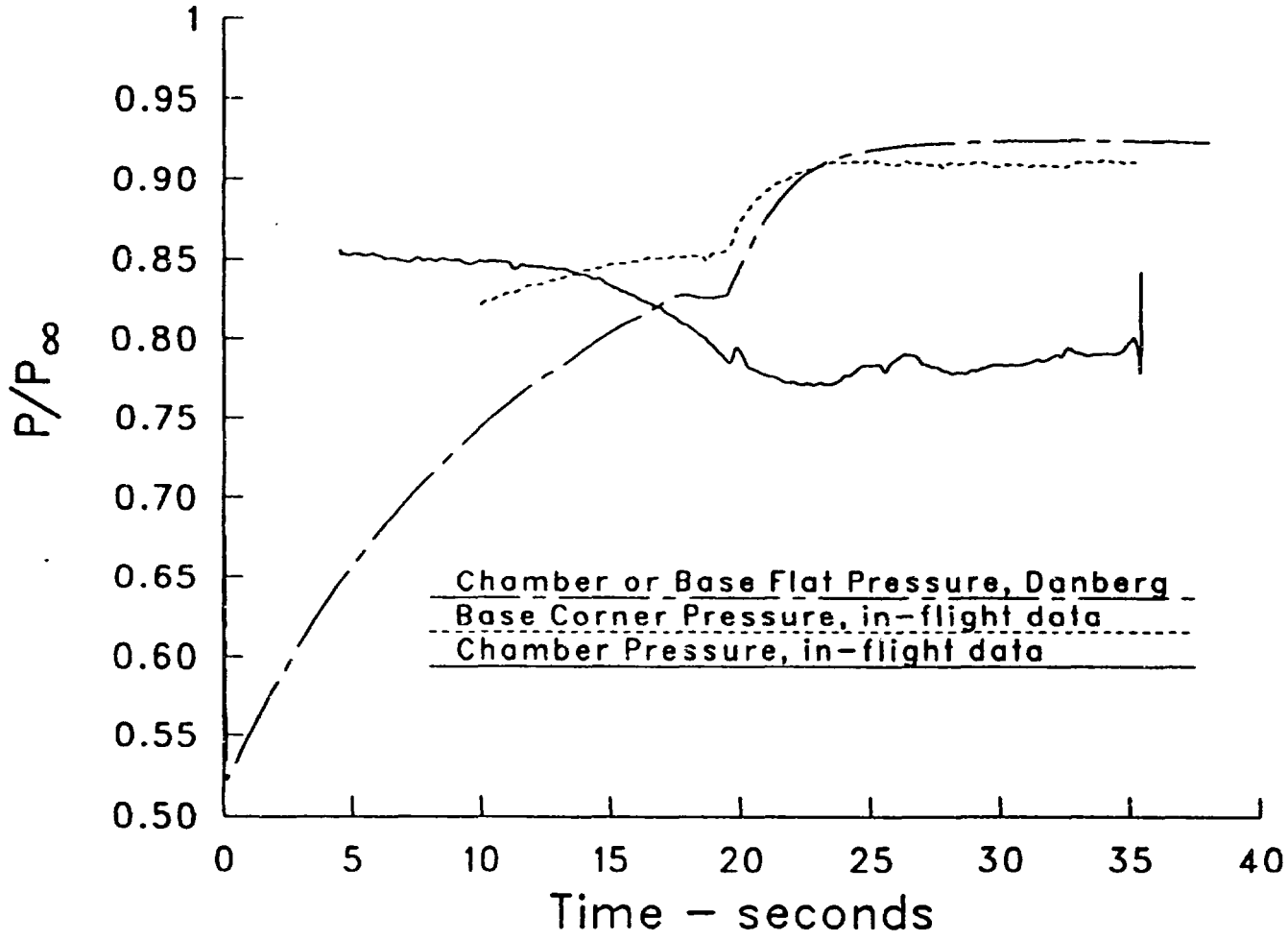

Figure 16: Flight 5—Base Corner, Chamber Pressures, Measured and Computed

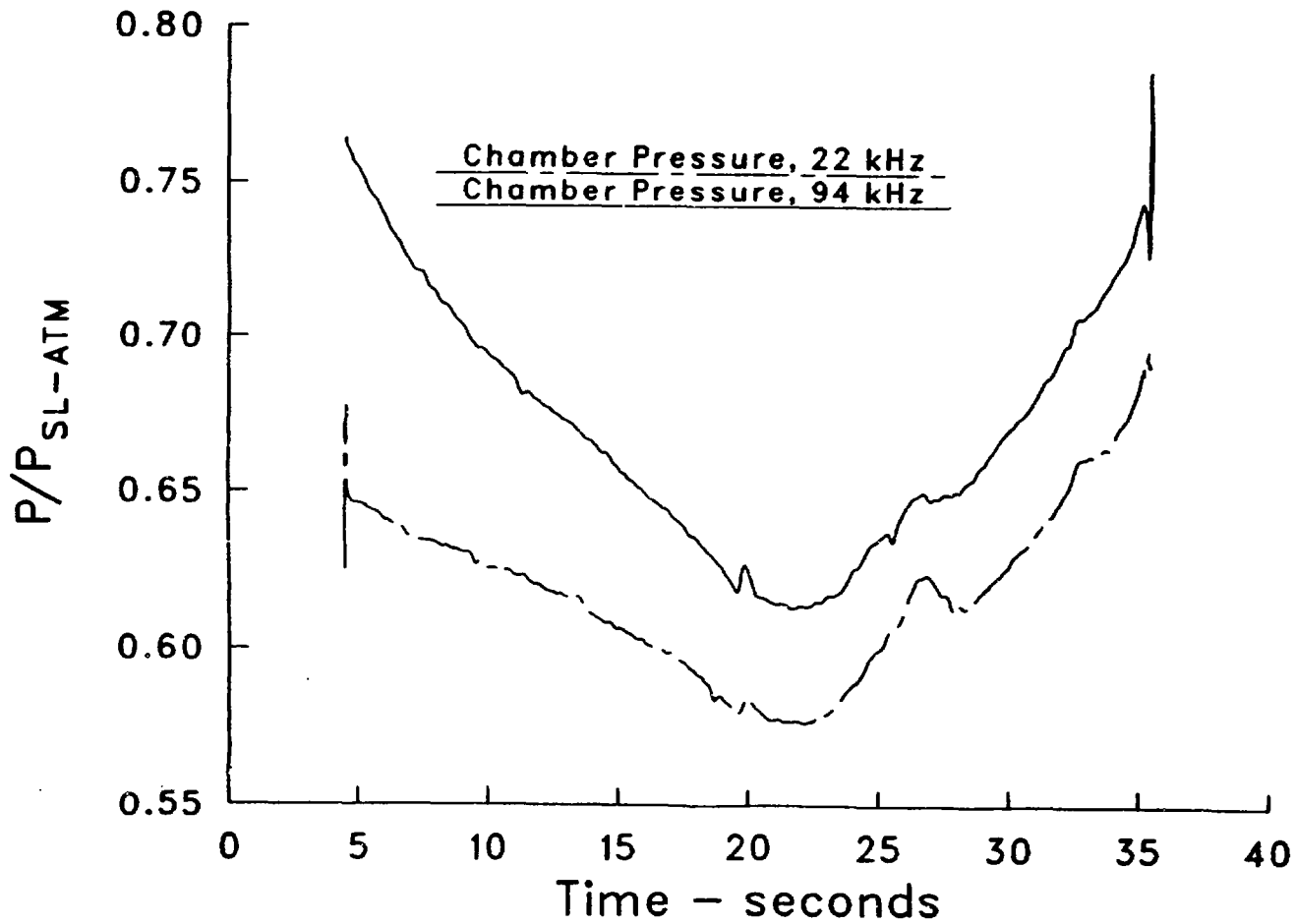

Figure 17: Flight 5—22 kHz and 94 kHz Chamber Pressures

APPENDIX A.

Assessment of Instrumentation Performance

1.0 INTRODUCTION

Due to some instrumentation failures and poor quality data, a brief analysis and discussion is provided along with speculation as to the cause of some problems. The table on the following page is similar to that of Table 4 in the body of the report and is a summary of failures and successes. The term 'success' means that useful data were acquired but does not necessarily imply good accuracy. Measurement signals from each channel were fed into an amplifier circuit and the amplifier output was then fed into a voltage controlled oscillator (VCO). The oscillator frequency is perturbed over a range of ± 7.5 % of the center frequency; that corresponds to an amplifier output of 0.0 to 5.0 volts with the center frequency at 2.5 volts. The oscillator frequencies from all channels were mixed and the mixed signal was then used to modulate a 245 Mhz transmitter carrier frequency.

2.0 DISCUSSION OF FAILURES

Chamber Pressure

Chamber pressure measurements for the first three flights utilized only one pressure transducer with two signal conditioning channels that had VCO's (voltage controlled oscillators) operating at 22 kHz and 94 kHz frequencies connected to the transducer output. The table shows that for each flight one or the other measurement channels failed completely. Apparently an imbalance or interaction between the two channels caused the failures, but the nature of the interaction is not understood. When one channel failed, the other channel was no longer affected and it then functioned normally. For flights 4 & 5, each channel was supplied with its own transducer and successful measurements were obtained on both frequencies.

Base Pressures

Base pressures were measured at two locations on the base. The 30 kHz channel measured the pressure in the small radius corner toward the outer radius of the base. The 40 kHz channel measured the pressure on the base flat near the propellant exit orifice. An RTV seal was placed between the pusher plate and the base to provide protection against the high pressure gases in the gun chamber. Results from flight 1 & 2 seemed reasonable but for flight 3, the 40 kHz base flat results were erratic and unreasonable for the first 47 seconds of the flight. After 47 seconds the channel seemed to function normally. It

Flight:	1	2	3	4	5
22 kHz Chamber	No data	No data	Full Flt	$\geq$18 sec	Full Flt
30 kHz Base Corner	Full Flt	Full Flt	Full Flt	No Data	$\geq$ 10 sec
40 kHz Base Flat:	Full Flt	Full Flt	$\geq$ 55 sec	4-10 sec	No Data
56 kHz Temp.	Full Flt	$\leq$ 22 sec	$\leq$ 20 sec	No Data	No Data
70 kHz Yawsonde	Partial Flt	Partial Flt	No Data	Full Flt	Full Flt
94 kHz Chamber	$\geq$4 sec	$\leq$ 22 sec	Full Flt	Full Flt	$\geq$5 sec
124 kHz Nose Cone	Full Flt	Full Flt	Full Flt	No Data	No Data

Table 1. Successful Measurements

was speculated that as the projectile exits the muzzle, the pusher plate starts to separate, and high pressure gun gases exiting the base propellant chamber might have overloaded the transducer. For this reason, the hole in the pusher plate was enlarged to the same diameter as the the base orifice so that gases could vent more freely. The table shows that base pressures (30 & 40 kHz channels) for flights 4 & 5 gave poorer result than for previous flights which indicates that enlargement of the pusher plate hole might have been a mistake.

Chamber Temperature

Chamber temperature was measured with the 56 kHz channel. This measurement was considered high risk but good results were obtained from spin fixture ground tests and were therefore attempted for the flight tests. The thermocouple was inserted through a hole drilled in the base wall which separated the instrumentation from the propellant. The thermocouple extended about 5 mm into the propellant cavity and was located in a small gap between the propellant grain and the igniter housing. The close proximity to the base wall and the igniter housing would affect the junction temperature due to radiation. Sporadic fluctuations observed from the ground tests seemed to indicate an insulating effect from periodic buildup and shedding of propellant residue. Results from the first flight were reasonable but no data were obtained from flights 4 & 5. Reasonable results were obtained for the first 22 seconds of flight 2 and for the first 20 seconds of flight 3. It is believed that the thermocouple for flight 2 failed at 22 seconds, leaving an open circuit which caused the failure of the 94 kHz chamber pressure at the same time (see Figure 3 or 4). The 56 kHz and 94 kHz channels utilized the same circuit board and had some common components. A modification to the circuit, which involved adding a resistor between the the amplifier input and ground, was made for flights 4 & 5. The purpose of this modification was to prevent an open-circuit floating voltage and was apparently successful because reasonable chamber pressure results, from the 94 kHz channel, were received for flights 4 & 5, even though the thermocouple failed and no useful temperatures were obtained.

Yawsonde Signals

Yawsonde signals were measured with the 70 kHz channel. For flight 1 & 2, results were obtained for about 1/3 of the flight and no results were obtained for flight 3. For flight 4 & 5, good results were obtained for the entire flight. There was some difficulty in mounting the sensors in the thin wall of the projectile nose and with the potting process – this problem therefore seems to be of a mechanical nature. The good results from flights 4 & 5 at more severe launch conditions support this conjecture. A significant advantage of the yawsonde measurement is that the primary parameter needed is the time interval between sun sensor pulses. A shift in VCO frequency or a moderate change in output voltage does not affect the quality of data.

Nose Cone Pressures

Nose cone pressures were measured with the 124 kHz channel. Results from the first flight seemed reasonable and results from flights 2 & 3 gave the correct trends but there appeared to be a substantial offset in absolute values. No useful data were received from flight 4 & 5. Since the nose cone transducers were not located in the area of high pressure gun gases, results as good or better than those from base pressure measurements were anticipated. If excess pressure was not a factor, then high acceleration forces would seem to be the cause of the nose cone problems

3.0 GENERAL DISCUSSION

O-Ring Seals

The O-ring seals that connected the base and base-closure pressure channels were an area of definite concern. Parker 2-003 (4.5mm OD) O-rings made from 'Buna N' rubber were used. Conventional O-ring seals are suitable for pressures of 1000-2000 psi which is far less than the maximum chamber pressures during launch. It was hoped that leakage past the O-rings during the high pressure transient would not be sufficient to load the transducers to more than 1000 psia. The quality of these O-ring appears to be sufficient at the M4A2 5W to 6W charges, but because of problems at the higher charges, it is not known if the seal was adequate.

RTV Base Seal

The RTV seal between the base and pusher plate was at least partially successful. Enlargement of the hole in the pusher plate for flights 4 & 5 may have caused the poor base pressure results for those flights. The hole was required so that gun gases could reach the chamber and ignite the propellant. If a hole was not required, it is believed that the RTV seal would have been highly successful. The chamber pressure transducers were protected by placing a small fitting into the orifice which was located inside the chamber. Magnesium-teflon igniter material was forced into the fitting at the equivalent of about 50,000 psia. As the igniter material burned out, the transducer was free to measure the chamber pressure.

Electronic Circuitry

Electronics for base pressures, chamber pressure and chamber temperature were located in the canister near the base. The signals were mixed, and brought forward to the noses section across the spring loaded connector, mixed with the nose cone pressure and yaw-sonde signals, and then sent to the transmitter located in the tip of the projectile nose. For all flights, signals were received from both the base section and the nose cone section. Generally, the electronics performed well with the exception of the transducers. Even when no useful measurements were obtained, shorting pulses were transmitted which indicate that signal conditioning, conversion to frequency (VCO's), and RF transmission was functioning properly.

Shorting Pulses

The output of the transducers were shorted for a period of about 40 msec at 10 sec intervals. The result was that for the 40 msec time period the the gage voltage was essentially zero. If drift in the circuit occurred downstream of the transducer, the shorting pulse would have given a measure of the drift. However any zero shift or drift in the transducer would not be detected. In a number of instances, the data gave the correct trends but the absolute values seem to have an offset error. The data indicate that most of the zero shift occurred within the transducer. For flights 2 & 3, shorting pulses were not received on some channels which indicated that the solid state shorting switch had failed.

Spring Loaded Connector

All signals from the base region were transmitted across a spring loaded connector to the nose section and transmitter. There was some apprehension as to the suitability of this connection but there was no indication of problems on any of the five flights.

Pressure Transducers

The predominant problem, concerning failures or zero-shifts, seems to be with the transducer. After the hole in the pusher plate was enlarged, base pressure results were worse – possibly indicating an excess pressure problem. The nose cone pressure results were disappointing and transducers should not have been exposed to high gas pressures, which suggests that acceleration forces may have caused the problem. Because of the two different reasons just mentioned for possible failures, it is not clear whether high acceleration forces or excess gun pressures, or both, were the primary cause of the failures. The Kulite transducers have a low sensitivity to acceleration loads but the limit on acceleration forces for which catastrophic failure would occur could not be supplied by the Kulite Corporation. The transducers should be tested before further tests at high zone launch conditions are conducted. Spin testing of the transducers could be accomplished on the LFD spin fixture by mounting the transducer off center and its axis normal to the spin axis. Centrifugal accelerations up to 15000 g should be attainable.

4.0 CONCLUSIONS

- Overall, the electronic circuitry performed well.
- The major problem is believed to be transducer failure or large zero shifts. Failures could have been caused by pressure overload or by high acceleration forces; but, which of these cause the difficulty could not be discerned.
- Transducer integrity needs to be determined before in-flight testing of projectiles with complex instrumentation.
- Contamination of the thermocouple junction along with radiation losses prevented accurate measurements. The thermocouples could not withstand the more severe launch condition and such failures were not unexpected.
- The Yawsonde problems were mechanical and no difficulty in future tests is anticipated.

INTENTIONALLY LEFT BLANK.

No of Copies	Organization
2	Administrator Defense Technical Info Center ATTN: DTIC-DDA Cameron Station Alexandria, VA 22304-6145
1	HQDA (SARD-TR) WASH DC 20310-0001
1	Commander US Army Materiel Command ATTN: AMCDRA-ST 5001 Eisenhower Avenue Alexandria, VA 22333-0001
1	Commander US Army Laboratory Command ATTN: AMSLC-DL Adelphi, MD 20783-1145
2	Commander US Army, ARDEC ATTN: SMCAR-IMI-I Picatinny Arsenal, NJ 07806-5000
2	Commander US Army, ARDEC ATTN: SMCAR-TDC Picatinny Arsenal, NJ 07806-5000
1	Director Benet Weapons Laboratory US Army, ARDEC ATTN: SMCAR-CCB-TL Watervliet, NY 12189-4050
1	Commander US Army Armament, Munitions and Chemical Command ATTN: SMCAR-ESP-L Rock Island, IL 61299-5000
1	Director US Army Aviation Research and Technology Activity ATTN: SAVRT-R (Library) M/S 219-3 Ames Research Center Moffett Field, CA 94035-1000

No of Copies	Organization
1	Commander US Army Missile Command ATTN: AMSMI-RD-CS-R (DOC) Redstone Arsenal, AL 35898-5010
1	Commander US Army Tank-Automotive Command ATTN: AMSTA-TSL (Technical Library) Warren, MI 48397-5000
1	Director US Army TRADOC Analysis Command ATTN: ATRC-WSR White Sands Missile Range, NM 88002-5502
(Class. only) 1	Commandant US Army Infantry School ATTN: ATSH-CD (Security Mgr.) Fort Benning, GA 31905-5660
(Unclass. only) 1	Commandant US Army Infantry School ATTN: ATSH-CD-CSO-OR Fort Benning, GA 31905-5660
1	Air Force Armament Laboratory ATTN: AFATL/DLODL Eglin AFB, FL 32542-5000
	Aberdeen Proving Ground
2	Dir, USAMSAA ATTN: AMXSY-D AMXSY-MP, H. Cohen
1	Cdr, USATECOM ATTN: AMSTE-TD
3	Cdr, CRDEC, AMCCOM ATTN: SMCCR-RSP-A SMCCR-MU SMCCR-MSI
1	Dir, VLAMO ATTN: AMSLC-VL-D

No. of
Copies Organization

2 Project Manager - Howitzer
Improvement Program
US Army, ARDEC
ATTN: AMCPM-HIP,
R. Kantenwein
R. DeKleine
Picatinny Arsenal, NJ 07806-5000

2 PEO-Armaments
Project Manager
Autonomous Precison-Guided
Munitions (APGM)
US Army, ARDEC
ATTN: AMCPM-APGM,
J. Williams
D. Griggs
Picatinny Arsenal, NJ 07806-5000

1 Program Executive Office for Armaments
US Army, ARDEC
ATTN: AMCPEO-AR-M, Mr. M. DellaTerga
Picatinny Arsenal, NJ 07806-5000

3 Commander
US Army, ARDEC
ATTN: SMCAR-FSA-M,
F. Brody
R. Botticelli
P. Demasi
Picatinny Arsenal, NJ 07806-5000

2 Commander
US Army, ARDEC
ATTN: SMCAR-AET-A,
R. Kline
H. Hudgins
Picatinny Arsenal, NJ 07806-5000

2 Commander
US Army, ARDEC
ATTN: SMCAR-FSP-A,
F. Scerbo
J. Bera
Picatinny Arsenal, NJ 07806-5000

1 Commander
US Army Missile Command
ATTN: AMSMI-RDK, W. Dahlke
Redstone Arsenal, AL 35898-5010

No. of
Copies Organization

1 Commander
Naval Surface Warfare Center
ATTN: Dr. W. Yanta,
Aerodynamics Branch
K-24, Bldg. 402-12
White Oak Laboratory
Silver Spring, MD 20910

1 Director
National Aeronautics and
Space Administration
Ames Research Center
ATTN: Dr. J. Steger
Moffett Field, CA 94035

1 Georgia Institute of Technology
The George W. Woodruff School of
Mechanical Engineering
ATTN: Dr. G. P. Neitzel
Atlanta, GA 30332-0405

1 EPR
ATTN: Dr. J. D. Kuzan
P.O. Box 2180
Houston, TX 77252-2180

Aberdeen Proving Ground

Commander, CRDEC, AMCCOM
ATTN: SMCCR-RSP-A,
M. C. Miller
D. Olson
SMCCR-MU,
W. Dee
C. Hughes
D. Bomley

USER EVALUATION SHEET/CHANGE OF ADDRESS

This Laboratory undertakes a continuing effort to improve the quality of the reports it publishes. Your comments/answers to the items/questions below will aid us in our efforts.

1. BRL Report Number BRL-MR-3888 Date of Report January 1991

2. Date Report Received _____

3. Does this report satisfy a need? (Comment on purpose, related project, or other area of interest for which the report will be used.) _____

4. Specifically, how is the report being used? (Information source, design data, procedure, source of ideas, etc.) _____

5. Has the information in this report led to any quantitative savings as far as man-hours or dollars saved, operating costs avoided, or efficiencies achieved, etc? If so, please elaborate. _____

6. General Comments. What do you think should be changed to improve future reports? (Indicate changes to organization, technical content, format, etc.) _____

CURRENT ADDRESS

Name

Organization

Address

City, State, Zip Code

7. If indicating a Change of Address or Address Correction, please provide the New or Correct Address in Block 6 above and the Old or Incorrect address below.

OLD ADDRESS

Name

Organization

Address

City, State, Zip Code

(Remove this sheet, fold as indicated, staple or tape closed, and mail.)

---FOLD HERE---

DEPARTMENT OF THE ARMY
Director
U.S. Army Ballistic Research Laboratory
ATTN: SLCBR-DD-T
Aberdeen Proving Ground, MD 210[illegible]-5066
OFFICIAL BUSINESS

NO POSTAGE
NECESSARY
IF MAILED
IN THE
UNITED STATES

BUSINESS REPLY MAIL
FIRST CLASS PERMIT No 0001, APG, MD

POSTAGE WILL BE PAID BY ADDRESSEE

Director
U.S. Army Ballistic Research Laboratory
ATTN: SLCBR-DD-T
Aberdeen Proving Ground, MD 21005-9989

---FOLD HERE---